





## Article

# Perils of Underestimating Species Diversity: Revisiting Systematics of *Psammocambeva* Catfishes (Siluriformes: Trichomycteridae) from the Rio Paraíba do Sul Basin, South-Eastern Brazil †

Wilson J. E. M. Costa \* , José Leonardo Mattos, Paulo J. Vilaro , Pedro F. Amorim  and Axel M. Katz 

Laboratory of Systematics and Evolution of Teleost Fishes, Institute of Biology, Federal University of Rio de Janeiro, Caixa Postal 68049, Rio de Janeiro CEP 21941-971, Brazil

\* Correspondence: wcosta@acd.ufrj.br

† LSID: zoobank.org:pub:288E0E4F-B644-4CD8-9775-094BAED4089B.

**Abstract:** *Psammocambeva*, a subgenus of *Trichomycterus* s.s., includes a clade endemic to south-eastern Brazil, the *Psammocambeva* alpha-clade (PAC), containing species with similar colour pattern and fin morphology, making difficult their identification without accurate examination. The greatest diversity of PAC species occurs in the Rio Paraíba do Sul basin area (RPSA), situated within the Atlantic Forest, one of the most important and endangered biodiversity centres in the world. Herein, we: perform a multigene phylogeny focusing on species of PAC; revise morphological characters diagnosing species of PAC from the RPSA, with special attention to those equivocally synonymised in a recent study; describe two new species, and provide a key for species identification. Molecular and morphological evidence supported the recognition of eight valid species belonging to four species complexes. Data indicated that *T. auroguttatus*, *T. travassosi*, and *T. longibarbatulus* are valid species. Finally, we discuss the negative impacts of underestimating species diversity in regions under the intense process of natural habitat loss, concluding that integrative approaches are important tools to estimate species diversity, but they should include a range of morphological characters informative to delineate and diagnose groups and their respective species, in association with phylogenies generated by robust molecular datasets.

**Keywords:** Atlantic Forest; comparative osteology; mountain biodiversity; multigene phylogeny; new species; species conservation



**Citation:** Costa, W.J.E.M.; Mattos, J.L.; Vilaro, P.J.; Amorim, P.F.; Katz, A.M. Perils of Underestimating Species Diversity: Revisiting Systematics of *Psammocambeva* Catfishes (Siluriformes: Trichomycteridae) from the Rio Paraíba do Sul Basin, South-Eastern Brazil. *Taxonomy* **2022**, *2*, 491–523. <https://doi.org/10.3390/taxonomy2040032>

Academic Editor: Phillip Lobel

Received: 25 October 2022

Accepted: 4 December 2022

Published: 8 December 2022

**Publisher's Note:** MDPI stays neutral with regard to jurisdictional claims in published maps and institutional affiliations.



**Copyright:** © 2022 by the authors. Licensee MDPI, Basel, Switzerland. This article is an open access article distributed under the terms and conditions of the Creative Commons Attribution (CC BY) license (<https://creativecommons.org/licenses/by/4.0/>).

## 1. Introduction

Catfishes of the subfamily Trichomycterinae (hereafter trichomycterines) comprise the most diversified clade of the Trichomycteridae, as well as one of the most species-rich groups of Neotropical freshwater fishes [1,2]. With over 275 valid species [3], trichomycterines are typical inhabitants of fast-flowing streams of all major South American biogeographic regions, occurring from lowland areas to high mountains above 4000 m asl [4–6]. Over half of all trichomycterines are endemic to eastern South America, between northeastern and southern Brazil, where they are represented by four genera: *Cambeva* Katz, Mattos and Costa 2018; *Ituglanis* Costa and Bockmann 1993; *Scleronema* Eigenmann 1917, comprising two subgenera, *Plesioscleronema* Costa, Sampaio, Giongo, Almeida, Azevedo-Santos, and Katz 2022 and *Scleronema*; *Trichomycterus* Valenciennes 1832, with six subgenera, *Cryptocambeva* Costa 2021, *Humboldtglanis* Costa 2021, *Megacambeva* Costa 2021, *Paracambeva* Costa 2021, *Psammocambeva* Costa 2021, and *Trichomycterus* [1,7–9]. The genus *Trichomycterus* in this strict sense [1] (hereafter *Trichomycterus* s.s.) [7] comprises the type species of the genus, *Trichomycterus nigricans* Valenciennes 1832, and about 60 valid species.

Among the subgenera of *Trichomycterus* s.s., *Psammocambeva* has the greatest geographical distribution, occurring between the Rio de Contas basin and Rio Ribeira de Iguaçu

basin [7]. *Psammocambeva* is also the only subgenus that is not diagnosable by unambiguous morphological characters, although being strongly supported by molecular data [7]. Species of *Psammocambeva* frequently have a relatively long premaxilla, but this condition is not present in all species included in this subgenus, and it occurs in another subgenus [7]. The great external morphological similarity among some species of *Psammocambeva* imposes some difficulty to taxonomists using only colour pattern, morphometric data, and fin morphology, sometimes making necessary use of osteological features to accurately identify species and multigene molecular data to infer their relationships [7,10]. The best example is an assemblage of species from south-eastern Brazil sharing the presence of conspicuous dark brown spots arranged on the flank and dorsum, that are members of a well-corroborated clade [7] (hereafter the *Psammocambeva* alpha-clade, PAC). Species may be misidentified when using only external morphological characters by most of them having similar colour patterns and fin morphology, including identical ray counts, but some features of the external morphology and osteology, and molecular evidence indicate that they belong to different well-corroborated subclades [7]. The greatest concentration of PAC species occurs in the Rio Paraíba do Sul basin and adjacent coastal drainages, including smaller river coastal basins between the mouth of the Rio Paraíba do Sul and the eastern extremity of the Baía da Ilha Grande. This area, hereafter the Rio Paraíba do Sul Area (RPSA), shelters the greatest concentration of species of *Trichomycterus s.s.*, sometimes with four or five species of different subgenera occurring in a single area [7,11]. This area is situated within the Atlantic Forest, one of the most important biodiversity centres in the world [12]. On the other hand, the Rio Paraíba do Sul is situated close to the cities of Rio de Janeiro and São Paulo, the largest and the fourth largest city in South America, respectively, with the area concentrating numerous farms and industries, consequently making riverine habitats highly impacted by anthropic activities. Seven species of *Psammocambeva* are presently known to occur in RPSA, among which six species are members of PAC (see below), and one, *Trichomycterus largoperculatus* Costa & Katz, 2022, belongs to another subgeneric lineage [13].

#### *Historical Review of PAC Species in RPSA*

The oldest available name for species occurring in RPSA is *Trichomycterus goeldii* Boulenger, 1896, endemic to the Rio Piabonha drainage and neighbouring drainages of the middle Rio Paraíba do Sul basin. It was first collected by Swiss naturalist Emil August Göldi (1859–1917), who lived in Brazil between 1884 and 1907, then adopted the name Emílio Augusto Goeldi. He worked at Museu Nacional, Rio de Janeiro, between 1884 and 1890, and subsequently (1891–1892) he was director of Colonia Alpina, an establishment created with the function of welcoming and repatriating Swiss immigrants, a period that Goeldi intensely dedicated to the study of Natural Sciences [14]. Several specimens representing the local fauna and flora found in the Colonia Alpina were collected by Goeldi, who then sent a small freshwater fish collection to the British Museum (presently, Natural History Museum, London). Boulenger [15] described *T. goeldii* based on two syntype specimens collected in the Colonia Alpina, which is situated in the upper Rio Paquequer drainage, which is part of the Rio Piabonha drainage, with headwaters in the Serra dos Órgãos. During the 20th century, other four species were described from the Rio Paraíba do Sul basin: *Trichomycterus auroguttatus* Costa 1992, *Trichomycterus macrophthalmus* Barbosa and Costa 2012, *Trichomycterus puriventrus* Barbosa and Costa 2012, and *Trichomycterus travassosi* (Miranda Ribeiro 1949) [16–19]. Another species occurring in RPSA is a species formerly identified as *Trichomycterus 'zonatus'* (not *Trichomycterus zonatus* (Eigenmann 1918)) in Katz et al. [1] or *Trichomycterus alternatus* (Eigenmann, 1917) in Reis and de Pinna [20]. Our studies have shown that the name *Trichomycterus jacupiranga*, Wosiacki & Oyakawa, 2005, is applicable to this geographically widespread species, found in a broad geographical range along the coastal basins of south-eastern Brazil (Vilardo et al. unpublished). Finally, we have found two still undescribed species in RPSA, one in the upper Rio Pomba drainage,

Rio Paraíba do Sul basin, and another in a small coastal stream connected to the Lagoa de Saquarema system.

Whereas a previous version of this study was being prepared for submission, a new paper on the taxonomy of *Trichomycterus* from the Rio Doce basin was published [21], in which two species of *Psammocambeva* from RPSA, *T. auroguttatus*, and *T. travassosi*, were considered synonyms of *T. alternatus*. These synonymies were proposed without explicit justification, besides omitting data on the anatomy and phylogenetic relationships contradicting such a proposal, that is available in the literature [7,10,22]. The objectives of this paper are: to perform a multigene phylogeny focusing on species of PAC, to revise morphological characters clearly, and unambiguously diagnose the species of PAC from the RPSA, with special attention to those equivocally synonymised by Reis & de Pinna [21], to describe the two new species, to provide a key for identification of species of *Psammocambeva* from the RPSA, and to discuss the negative impacts of underestimating species diversity in regions under the intense process of natural habitat loss.

## 2. Materials and Methods

### 2.1. Specimens

Specimens used in this study comprised both those previously deposited in ichthyological collections and those collected in recent field studies using small dip nets (40 × 30 cm), with collecting permits given by ICMBio (Instituto Chico Mendes de Conservação da Biodiversidade; permit numbers: 38553-13, 48432-9, 50247-9, 71309-3) and INEA (Instituto Estadual do Ambiente, Rio de Janeiro; permit number: 037-2018). Euthanasia was conducted using a buffered solution of tricaine methane sulphonate (MS-222) at a concentration of 250 mg/L, following AVMA (American Veterinary Medical Association) Guidelines [23] and the European Commission DGXI consensus for fish euthanasia [24,25], thus following methods approved by CEUA-CCS-UFRJ (Ethics Committee for Animal Use of Federal University of Rio de Janeiro; permit number: 065/18). Specimens used in morphological studies were first fixed in formalin for two weeks and then placed in 70% ethanol. Specimens cleared and stained for osteological analyses were preserved in glycerine. Specimens used in the molecular analysis were fixed and preserved in absolute ethanol. In lists of specimens, the abbreviation C&S indicates specimens that were cleared and stained for osteological analyses, and the abbreviation DNA indicates specimens directly fixed and preserved in absolute ethanol for molecular analyses. Most material used in this study is deposited in the Instituto de Biologia, Universidade Federal do Rio de Janeiro (UFRJ), but some specimens are also deposited in the Centro de Ciências Agrárias e Ambientais, Universidade Federal do Maranhão (CICCAA), Field Museum of Natural History, Illinois (FMNH), Natural History Museum, London (BMNH), Museu Nacional, Universidade Federal do Rio de Janeiro (MNRJ), and Museu de Zoologia, Universidade de São Paulo (MZUSP). Material of new species is listed above species descriptions, where geographical names follow Portuguese regional terms. Material of other species is listed in Appendix A.

### 2.2. Morphological Data

Measurements were expressed as a percent of the standard length (SL), or head length when involving head parts, and were made using landmarks described by Costa [17] and modified by Costa et al. [26]. Fin-ray counts, and formulae followed Bockmann and Sazima [27], modified by Costa et al. [26], with lowercase Roman numerals indicating procurrent unsegmented unbranched rays of unpaired fins, uppercase Roman numerals indicating segmented unbranched rays of any fin, and Arabic numerals indicating segmented branched rays of any fin. Vertebra and rib counts were made in cleared and stained specimens and radiographs; vertebra counts did not include the Weberian Apparatus and the compound caudal centrum was counted as a single element. The methodology for clearing and staining specimens followed Taylor and Van Dyke [28]. Osteological illustrations were primarily made in a stereomicroscope Zeiss Stemi SV 6 with camera lucida. Terminology

for osteological structures is according to Costa [7] and for pores of the latero-sensory system, to Arratia and Huaquin [29], modified by Bockmann and Sazima [27].

### 2.3. DNA Extraction, Amplification, and Sequencing

Genomic DNA extract was obtained from caudal peduncle muscle tissue using DNeasy Blood & Tissue Kit (Qiagen). DNA quality and molecular weight of the samples were evaluated by Agarose gel electrophoresis. The polymerase chain reaction (PCR) method was used to amplify the target DNA fragments used in this study. PCR primers used were: Cytb Siluri F and Cytb Siluri R [30], CatThr29 and Glu 31 [31], and Glu 5 and Cb23 [32] for the mitochondrial gene cytochrome b (CYTB); FISHF1 and FISHR1 [33] for the mitochondrial gene cytochrome c oxidase I (COX1); MHRAG2-F1 and MHRAG2-R1 [34], RAG2 TRICHO F and RAG2 TRICHO R [35], and RAG2 MCF and RAG2 MCR [36] for the nuclear gene recombination activating 2 (RAG2); MYH6 TRICHO F and MYH6 TRICHO R [35], and myh6\_F459 and myh6\_R1322 [37] for the nuclear gene myosin heavy chain 6 (MYH6). The PCR reactions were made in 60 µL with the following reagents concentrations: 5× GreenGoTaq Reaction Buffer (Promega), 3.0 mM MgCl<sub>2</sub>, 1 µM of each primer, 0.2 mM of each dNTP, 1 u of Promega GoTaq Hot Start polymerase and 50 ng of total genomic DNA. Negative controls were used to check for contaminants in all those reactions. The thermocycling profile was: initial denaturation for 2–5 min at 94–95 °C; 35 cycles of denaturation for 1 min at 94–95 °C, annealing for 0.5–1 min at 45–55 °C and extension for 1–1.2 min at 72 °C; and terminal extension for 7 min at 72 °C. The PCR products were purified using the Wizard SV Gel and PCR Clean-Up System (Promega). Sequencing reactions were made using the BigDye Terminator Cycle Sequencing Mix (Applied Biosystems). Cycle sequencing reactions were performed in 20 µL reaction volumes containing 4 µL BigDye, 2 µL sequencing buffer 5× (Applied Biosystems), 2 µL of the amplified products (20–40 ng), 2 µL primer and 10 µL deionized water. The thermocycling profile was as follows: (1) 35 cycles of 10 s at 96 °C, 5 s at 54 °C, and 4 min at 60 °C. Edition of the sequences and evaluation of chromatograms were performed using MEGA 11 [38]. To verify the correct codification of each sequence, and the absence of premature stop codons or indels, the DNA sequences were translated into amino acid residues using the program MEGA 11.

### 2.4. Phylogenetic Analyses

Terminal taxa comprised all eight species of PAC from RPSA, including the two new species, besides six other species of PAC representing different lineages. This taxon sample included all species of PAC. Outgroups were three species of *Psammocambeva* not included in PAC; nine species of *Trichomycterus* representing the other five subgenera; two trichomycterine species of the genera *Cambeva* and *Scleronema* representing the sister group of *Trichomycterus s.s.*; three trichomycterine species representing other sub familial lineages; four species representing other trichomycterid subfamilies; and one nematogenyid species, sister to the Trichomycteridae. GenBank accession numbers are provided in Appendix B. Each gene data set was aligned using MEGA 11 [38] through Clustal W [39] algorithm; stop codons and gaps were not found in the aligned molecular data set. The matrix with concatenated molecular data, 2974 bp (COX1 522 bp, CYTB 1088 bp, MYH6 543 bp, RAG2 821 bp), was submitted to the PartitionFinder2.1.1 [40] algorithm to obtain the best-fit partitions and models schemes, following the Corrected Akaike Information Criterion (AICc) (see Appendix C). Two independent phylogenetic reconstruction approaches were conducted, Bayesian Inference (BI) and Maximum Likelihood (ML). The BI was conducted using MrBayes 3.2.5 [41]. Two independent Markov chain Monte Carlo (MCMC) runs of two chains each for  $5 \times 10^6$  generations were run with a sampling frequency of every 1000 generations. The convergence of the MCMC chains and the proper burn-in value were determined by evaluating the stationary phase of the chains using the effective sample size with Tracer 1.7.1 [42]. The consensus tree and Bayesian posterior probabilities were calculated after removing the first 25% samples. The ML was calculated using IQTREE

2.2.0 [43], and the support value of the nodes was estimated by calculation of 1000 ultrafast bootstrap [44] and 1000 bootstrap [45] replicates. Gene trees (Appendix D) were generated using IQTREE 2.2.0.

### 3. Results

#### 3.1. Phylogenetic Relationships

Both phylogenetic analyses recovered monophyly of *Psammocambeva* and PAC with high support values, but several internal nodes were weakly supported, indicating a low phylogenetic signal (Figure 1). Species endemic to RPSA appear in four different subclades. Two of them, *T. auroguttatus* and *T. goeldii*, are supported as sister taxa, belonging to a clade here called the *T. goeldii* complex, also including *T. alternatus* and *T. astromycterus*, which is corroborated by morphological characters (see below). *Trichomycterus jacupiranga* is supported as a sister to *T. vinnulus*, forming a clade here called the *T. jacupiranga* complex. The two other clades here, called the *T. puriventris* and *T. travassosi* complexes, contain only species endemic to RPSA and are corroborated by morphological data (see below).

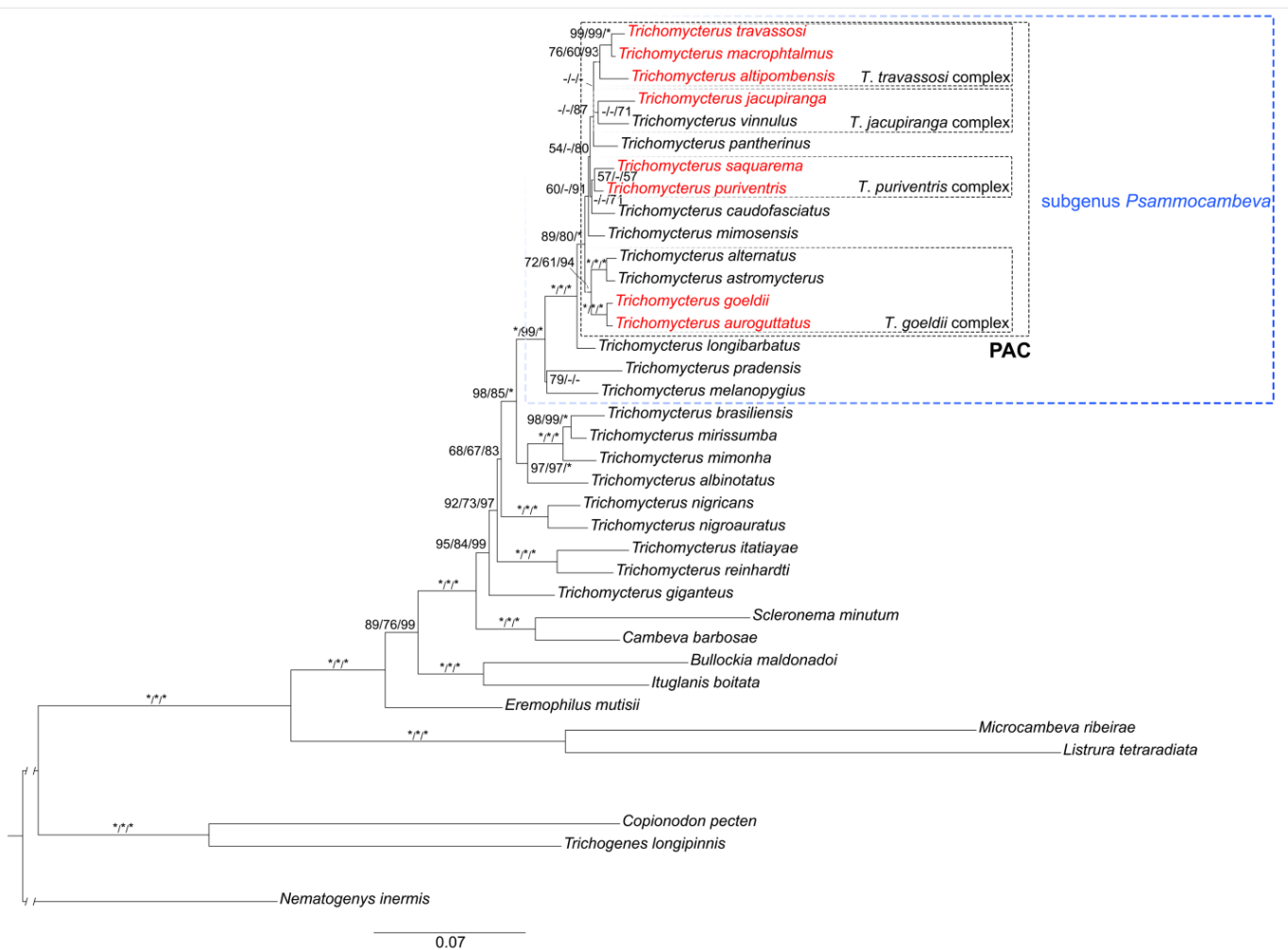


**Figure 1.** Maximum likelihood tree estimated by IQ-tree for 24 species of *Trichomycterus* and 10 outgroups, combining four genes (COI, CYTB, MYH6, and RAG2, with a total of 2974 bp). Taxa endemic to the Rio Paraíba do Sul Area are depicted in red. The numbers above branches indicate Bayesian posterior probabilities of the Bayesian inference analysis, bootstrap, and fast bootstrap values of the Maximum likelihood analyses, respectively, separated by a bar. Asterisks (\*) indicate maximum support values and dashes (-) indicate values below 50. PAC, *Psammocambeva* alpha-clade.

### 3.2. The *Trichomycterus goeldii* Complex

This clade comprises four species, two endemic to the Rio Paraíba do Sul basin, *T. auroguttatus*, and *T. goeldii*, and two presently known only from the Rio Doce basin, *T. alternatus* and *T. astromycterus* Reis, de Pinna and Pessali 2019 (Figure 1), thus corroborating previous studies [7,22]. According to Costa [7], the *T. goeldii* complex is supported by three osteological apomorphic conditions not found elsewhere among species of *Trichomycterus s.s.* that are herein confirmed: a long postero-lateral process of the autopalatine, its length nearly equal or slightly longer than the autopalatine longitudinal length excluding the postero-lateral process (Figure 2F in Costa [7]); a slightly folded maxilla (Figure 2F in Costa [7]); and the anterior cranial fontanel represented by a minute aperture (Figure 8B in Costa [7]). All these apomorphies are here confirmed. Among these morphological features, the most conspicuous are the first two, which are related to a highly modified mesethmoidal region, including a unique shape of the autopalatine with a long and robust postero-lateral process and a deep concavity on the medial margin, as well as a typical maxilla morphology, which is slightly folded and has a slight anterior expansion close to the middle area (Figure 2A,B). In all other species of *Psammocambeva*, the autopalatine and the maxilla exhibit different morphology (Figure 2C–H).

Molecular data highly supported the species pairs of each river basin, Rio Doce and Rio Paraíba do Sul basins, as monophyletic (Figure 1). The subclade endemic to RPSA comprising *T. auroguttatus* and *T. goeldii* is morphologically corroborated by both species sharing the presence of a robust comma-shaped osseous core in the autopalatine articular shell for the lateral ethmoid (Figure 2A,B), and a widened third hypobranchial, with its anterior extremity distinctively wider than the anterior extremity of the second hypobranchial (Figure 3A). These two conditions are not found elsewhere among congeners of *Psammocambeva* (Figures 2C–H and 3B,C). *Trichomycterus auroguttatus* and *T. goeldii* are also easily distinguished from *T. astromycterus* by the last species having caudal fin emarginate (vs. subtruncate), more principal dorsal-fin rays (10 or 11, vs. nine) and a shorter nasal barbel, its tip posteriorly not reaching orbit (vs. reaching area behind orbit). The phylogenetic analyses indicated that the *T. goeldii* complex is sister to a clade comprising all other species of PAC here analysed, which is weakly supported by molecular data and tentatively diagnosed by the presence of a small posterior expansion of the metapterygoid (Figure 4C–G), that is absent in species of the *T. goeldii* complex (Figure 4A) and other lineages of *Psammocambeva* (Figure 4B).

The two species endemic to the RPSA occur in two disjunct areas, both between about 800 and 1200 m asl, with *T. auroguttatus* being endemic to the upper Rio Preto drainage, a large left tributary to the Rio Paraíba do Sul basin, with headwaters in the Serra da Mantiqueira, and *T. goeldii* occurring in a broad area of the middle Rio Paraíba do Sul basin, with headwaters in the Serra do Mar (Figure 5). *Trichomycterus auroguttatus* (Figure 6) is distinguished from *T. alternatus* (Figure 7) and *T. goeldii* (Figure 8) by the presence of a shorter nasal barbel, its tip reaching area immediately posterior to orbit (vs. area just anterior to opercle); a larger eye that is always larger than the opercular patch of odontodes (vs. nearly equal in size); supraorbital canal usually interrupted, forming two separate segments, resulting in the presence of two s3 pores (Figure 9A; vs. supraorbital canal continuous, with a single s3 pore, Figure 9B); and brown spots of the anterior portion of a row of spots on the longitudinal midline of flank deeper than long, separated by broader interspaces, never forming a stripe (vs. longer than deep, separated among themselves by narrow interspaces, often coalesced to form a stripe). Whereas specimens of *T. auroguttatus* may have a single median s6 pore or two s6 pores in close proximity (Figure 9A), specimens of *T. goeldii* always have a single median s6 pore (Figure 9B). Finally, only in larger specimens of *T. auroguttatus*, above about 60 mm SL, the postero-lateral process of the autopalatine is proportionally longer and the medial margin of the autopalatine is sinuous (compare Figure 2A,B). Despite the diagnostic morphological characteristics here described, specific studies of species delimitation, in course by the authors, directed to several populations of

the clade including *T. auroguttatus* and *T. goeldii* are necessary to infer species limits and to validate their taxonomic status.

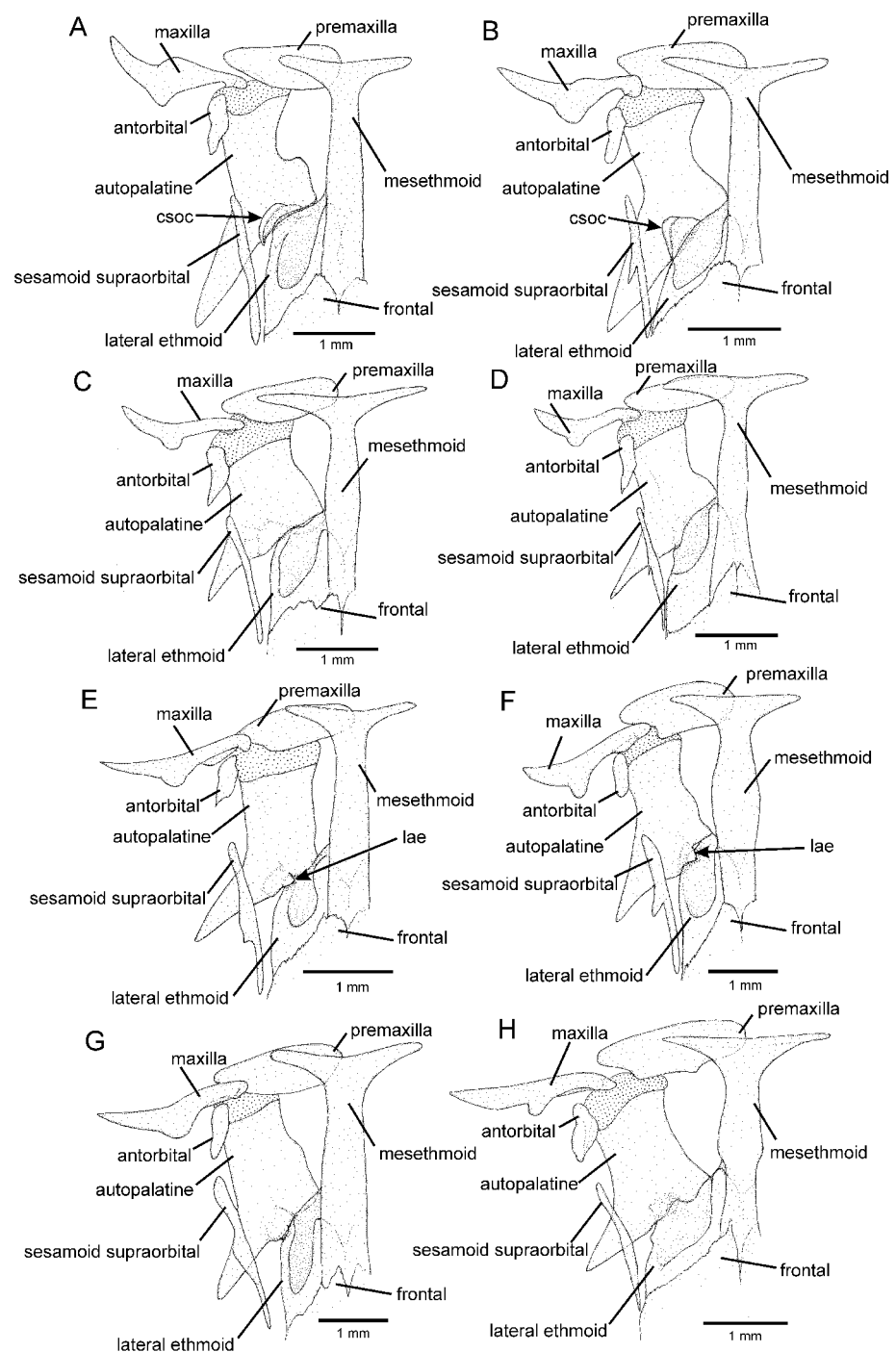


**Figure 2.** Mesethmoidal region, middle and left portions, dorsal view: (A) *Trichomycterus auroguttatus*; (B) *Trichomycterus goeldii*; (C) *Trichomycterus puriventris*; (D) *Trichomycterus saquarema* Costa, Katz, Vilardo and Amorim, sp. nov.; (E) *Trichomycterus travassosi*; (F) *Trichomycterus altipombensis* Costa, Katz, Vilardo and Mattos, sp. nov.; (G) *Trichomycterus jacupiranga*; (H) *Trichomycterus longibarbatu*s. Larger stippling represents cartilage. csoc, comma-shaped osseous core; lae, laminar articular expansion.

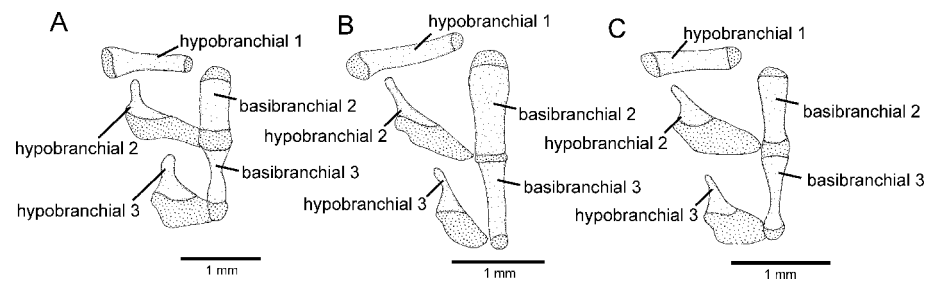


**Figure 3.** Partial ventral branchial skeleton, mid-left portion, dorsal view: (A) *Trichomycterus auroguttatus*; (B) *Trichomycterus jacupiranga*; (C) *Trichomycterus saquarema* Costa, Katz, Vilardo and Amorim, sp. nov. Larger stippling represents cartilages.

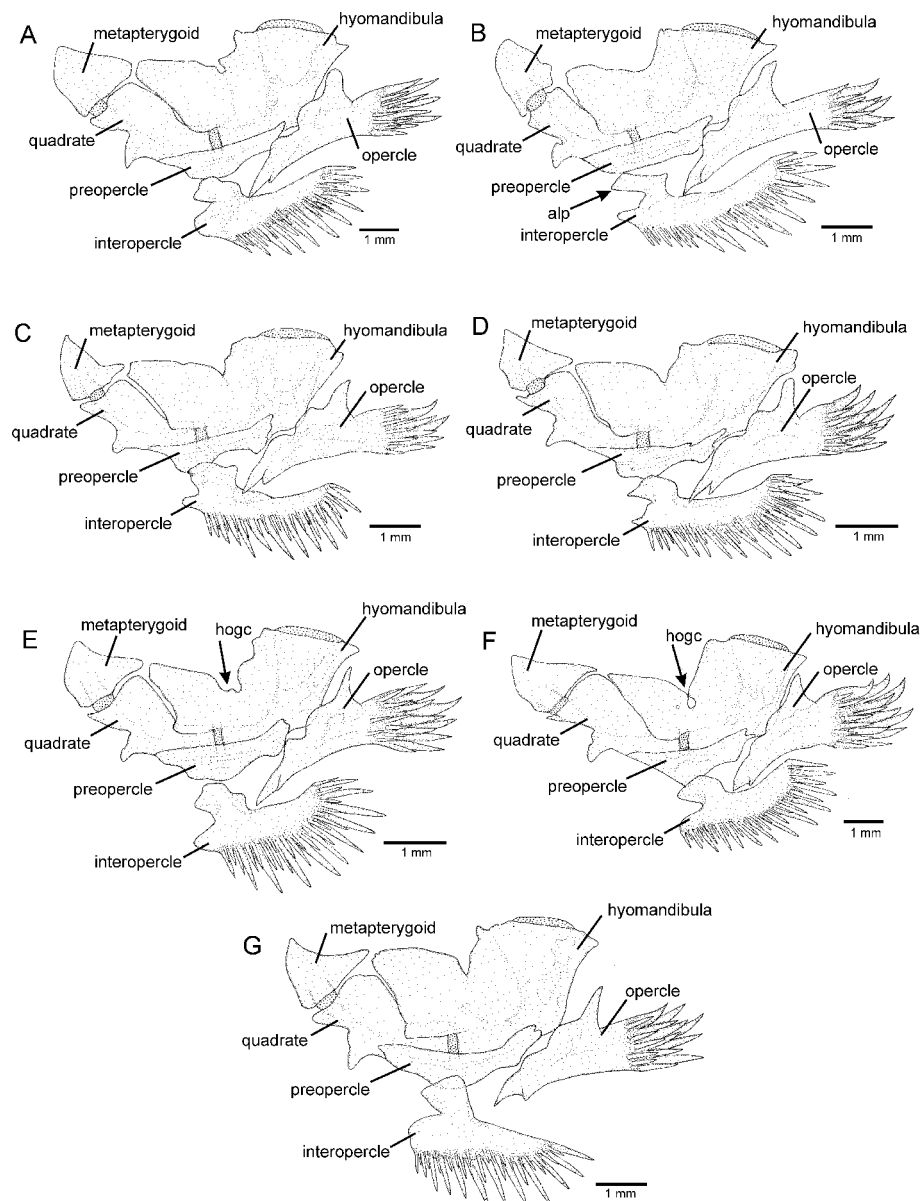


**Figure 4.** Left jaw suspensorium and opercular series, lateral view: (A) *Trichomycterus auroguttatus*; (B) *Trichomycterus longibarbatus*; (C) *Trichomycterus puriventris*; (D) *Trichomycterus saquarema* Costa, Katz, Vilardo and Amorim, sp. nov.; (E) *Trichomycterus travassosi*; (F) *Trichomycterus altipombensis* Costa, Katz, Vilardo and Mattos, sp. nov.; (G) *Trichomycterus jacupiranga*. Larger stippling represents cartilages. alp, axe-like process; hogc, hyomandibular outgrow cleft.



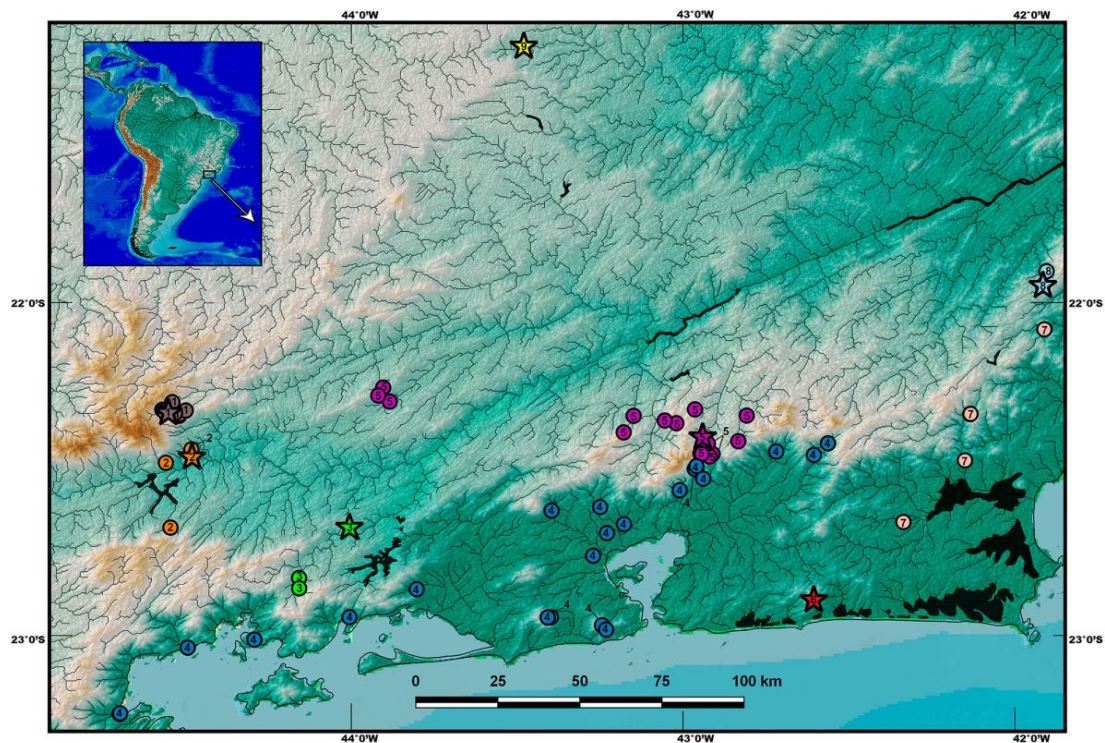


**Figure 5.** Geographical distribution of species of the *Psammocambeva* alpha-clade, genus *Trichomycterus*, in the Rio Paraíba do Sul Area: *T. altipombensis* Costa, Katz, Vilaro and Mattos, sp. nov. (9, yellow); *T. auroguttatus* (1, brown); *T. goeldii* (5, purple); *T. jacupiranga* (4, blue); *T. aff. jacupiranga* (7, pink); *T. macrophthalmus* (3, green); *T. puriventris* (8, light blue); *T. saquarema* Costa, Katz, Vilaro and Amorim, sp. nov. (6, red); *T. travassosi* (2, orange). Stars indicate type localities.

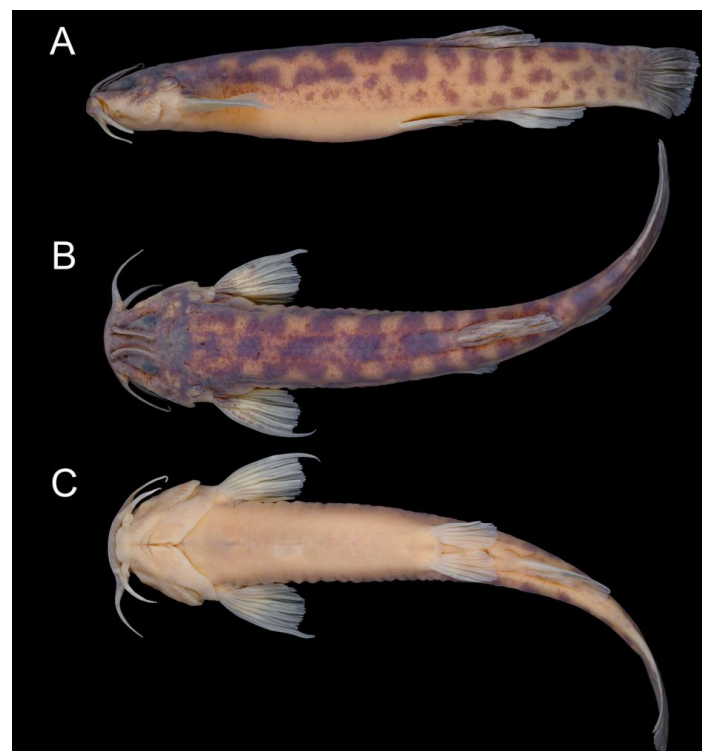


**Figure 6.** *Trichomycterus auroguttatus*, UFRJ 11675, topotype, 59.2 mm SL: (A) lateral, (B) dorsal, and (C) ventral views.



**Figure 7.** *Trichomycterus alternatus*, UFRJ 9900, 58.2 mm SL: (A) lateral, (B) dorsal, and (C) ventral views.

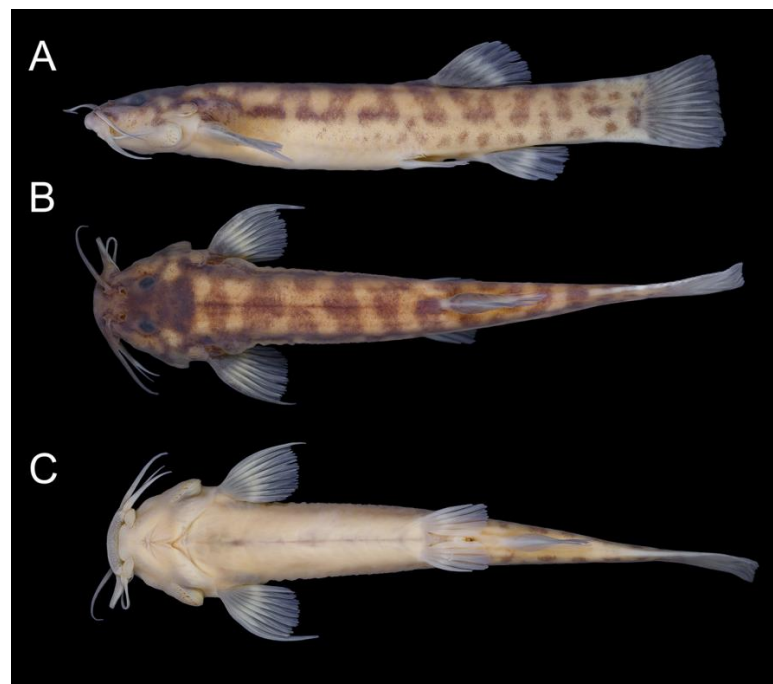


**Figure 8.** *Trichomycterus goeldii*, UFRJ 7938, topotype, 57.9 mm SL: (A) lateral, (B) dorsal, and (C) ventral views.

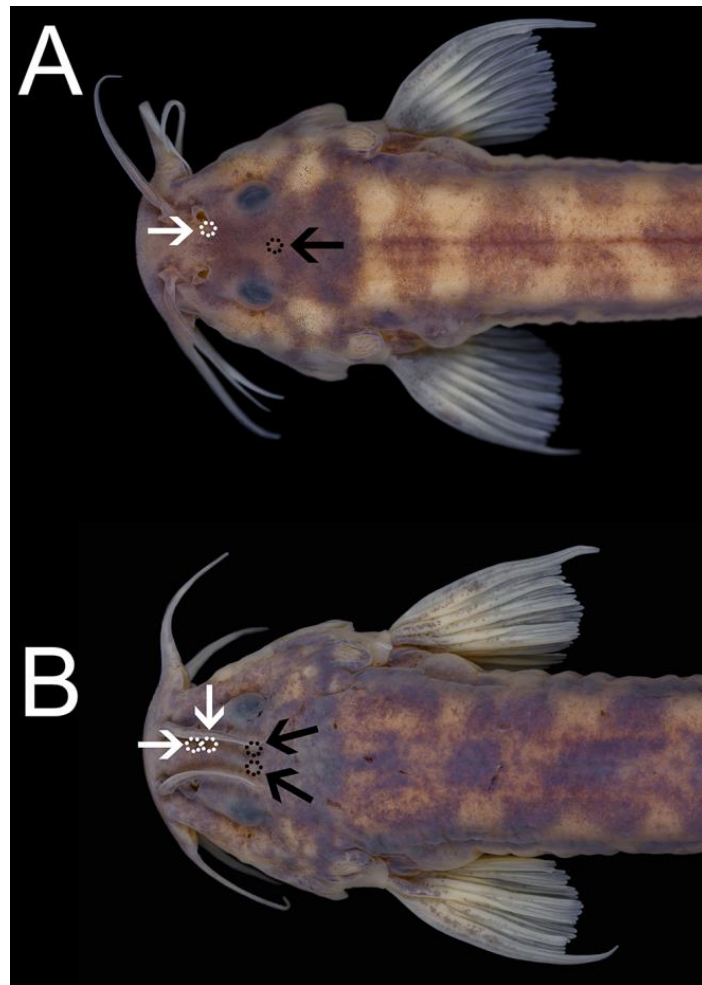


**Figure 9.** Head, dorsal view: (A) *Trichomycterus goeldii*, UFRJ 7938, 57.9 mm SL; (B) *Trichomycterus auroguttatus*, UFRJ 11675, 59.2 mm SL. Black arrows, S6 pores; white arrows, S3 pores.

*Trichomycterus longibarbatus* Costa 1992 (Figure 10), recently considered a synonym of *T. alternatus*, is not a member of the *T. goeldii* complex. Its autopalatine has a short posterolateral process and a weakly concave medial margin, and the premaxilla is not folded (Figure 2H). *Trichomycterus longibarbatus* is also distinguished from species of the *T. goeldii* complex and all other species of *Psammocambeva* by having longer barbels (Figure 10), with the nasal barbel reaching an area between the opercle and the pectoral-fin base, often reaching the middle portion of the pectoral-fin base (vs. reaching the middle portion of the opercle as in *T. alternatus* or an area anterior to it), and the maxillary barbel reaching an area posterior to the pectoral-fin base (vs. reaching the pectoral-fin base as in *T. alternatus* or more often an area anterior to it as in most other trichomycterids). In addition, *T. longibarbatus* differs from all other trichomycterine taxa from eastern South America by having a narrow and anteriorly expanded interopercular dorsal process, thus assuming an axe-like unique morphology (Figure 4B). It also differs from all other species of PAC by having a nearly straight premaxilla (Figure 2H). The present analysis indicates that *T. longibarbatus* is a sister to a clade including all species of PAC.

### 3.3. The *Trichomycterus jacupiranga* Complex

This clade, comprising *T. jacupiranga* and *T. vinnulus*, is weakly supported by molecular data and not corroborated by morphology. However, *T. jacupiranga*, *T. pantherinus*, and *T. vinnulus* share the presence of a second basibranchial that is longer than the third one (Figure 2B), whereas in other congeners the second basibranchial is nearly equal in length

or smaller than the third (Figure 2A,C,D), suggesting that *T. pantherinus* is also a member of this complex, although not supported by molecular data (Figure 1). Species of this group may exhibit high levels of colouration polymorphism. *Trichomycterus jacupiranga* (Figure 11), the only species of the complex occurring in RPSA, is a geographically widespread species. In RPSA, it is found in small coastal basins of western Rio Janeiro state, whereas populations here tentatively identified as *Trichomycterus* cf. *jacupiranga* are found in the coastal basins of eastern Rio Janeiro state (Figure 5) and are easily distinguished from congeners by having incisiform jaw teeth, instead of pointed or having a slightly rounded tip.



**Figure 10.** *Trichomycterus longibarbatus*, UFRJ 3368, topotype, 52.9 mm SL: (A) lateral, (B) dorsal, and (C) ventral views.

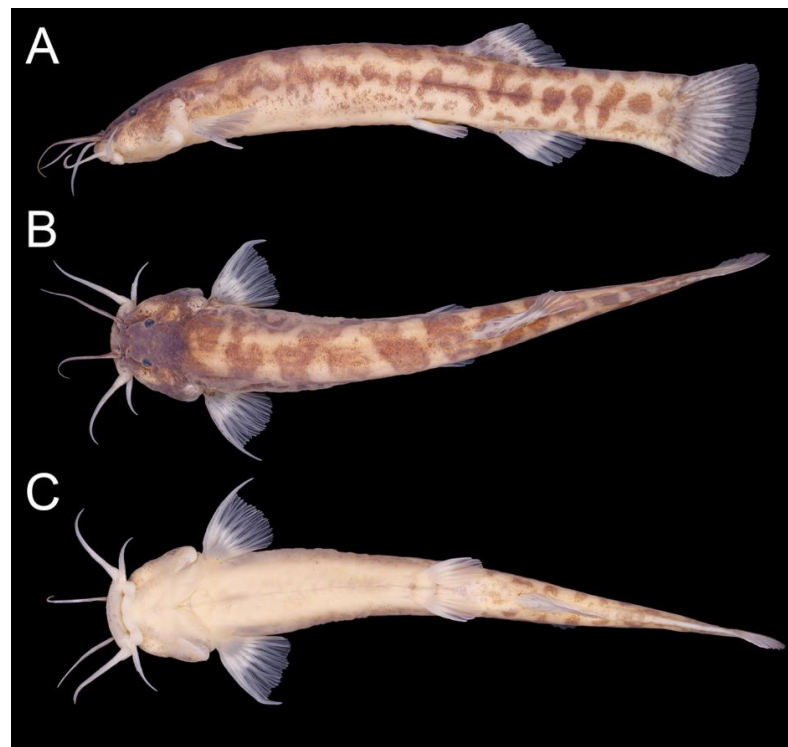


**Figure 11.** *Trichomycterus jacupiranga*, UFRJ 12781, 79.5 mm SL: (A) lateral, (B) dorsal, and (C) ventral views.

Species of the *T. jacupiranga* and *T. travassosi* complexes share the presence of a deep notch on the anterior outgrowth of the hyomandibula (Figure 4E–G), suggesting that these clades are sister groups. A notch or a deep concavity in this part of the hyomandibula commonly occurs in juveniles of species of *Trichomycterus s.s.*, but a persistent open notch in adults (Figure 4E–G), sometimes with margins partially fused, forming a rounded aperture (Figure 4F) is unique for this clade. In species of the *T. travassosi* complex, the entire hyomandibular outgrowth is attenuated, possibly consisting of an extra apomorphic condition (Figure 4E,F). In adults of other species of *Psammocambeva*, the notch is rudimentary (Figure 4A–D).

### 3.4. The *Trichomycterus puriventris* Complex

This clade, weakly supported by molecular data, is diagnosable by a unique colour pattern (see diagnosis for the new species below). It comprises two species: *T. puriventris* (Figure 12), endemic to the Rio Grande drainage, a tributary of the lower Rio Paraíba do Sul basin, in altitudes between about 300 and 600 m asl, and a new species (Figure 13), below described, endemic to the Lagoa de Saquarema system, found at about 100 m asl.



**Figure 12.** *Trichomycterus puriventris*, UFRJ 5398, paratype, 76.9 mm SL: (A) lateral, (B) dorsal, and (C) ventral views.

*Trichomycterus saquarema* Costa, Katz, Vilardo and Amorim, sp. nov.

LSID:urn:lsid:zoobank.org:act:BEC1AABD-8D41-4ABD-AD1D-869C23BE8204.

Figures 13 and 14, Table 1.

*Holotype.* UFRJ 13019, 53.1 mm SL; Brazil: Rio de Janeiro State: Saquarema Municipality: Rio Roncador, a tributary of the Lagoa de Saquarema, Universalismo road, 22°52'56" S 42°39'02" W, about 90 m asl; A. M. Katz & P. J. Vilardo, 5 September 2022.

*Paratypes.* UFRJ 13237, 2 ex. (C&S), 35.3–51.8 mm SL; UFRJ 13236, 2 ex., 13.9–32.0 mm SL; collected with holotype.—UFRJ 13059, 3 ex., 45.8–56.7 mm SL; UFRJ 13020, 2 ex. (C&S), 46.5–52.0 mm SL; UFRJ 12999, 2 ex. (DNA), 23.2–42.1 mm SL; CICCAA 07153; 2 ex., 32.2–35.4 mm SL; same locality as holotype; W.J.E.M. Costa et al., 4 July 2022.

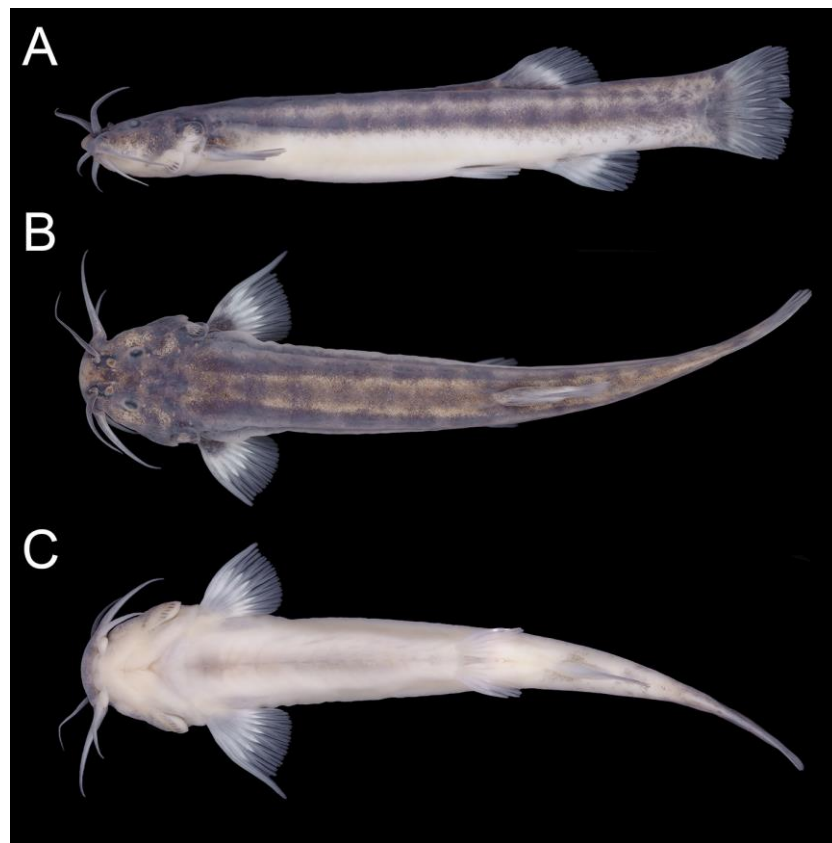


**Figure 13.** *Trichomycterus saquarema* Costa, Katz, Vilardo and Amorim, sp. nov., UFRJ 13019, holotype, 53.1 mm SL: (A) lateral, (B) dorsal, and (C) ventral views.

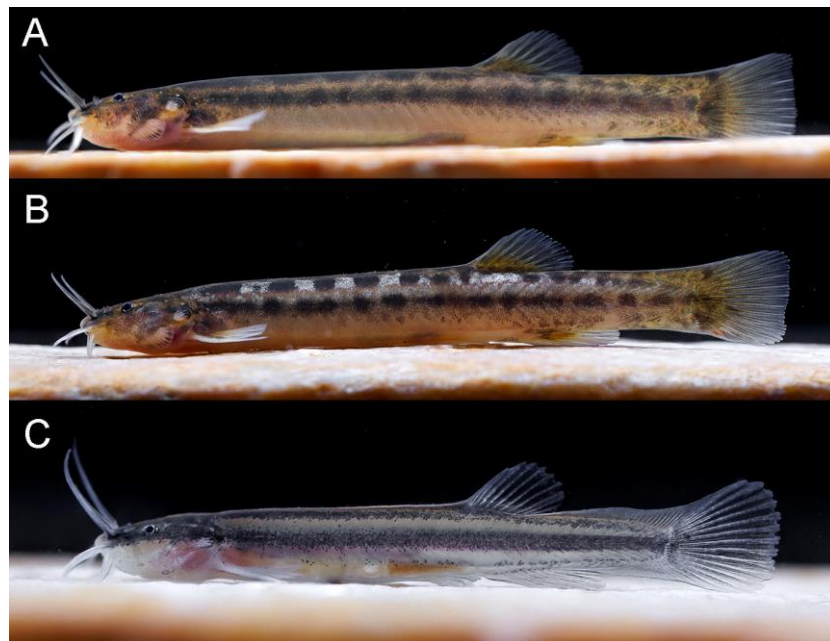


**Figure 14.** Live specimens of *Trichomycterus saquarema* Costa, Katz, Vilardo and Amorim, sp. nov. (A) UFRJ 13019, holotype, 53.1 mm SL; (B) UFRJ 13059, paratype, 45.8 mm SL; (C) UFRJ 13236, paratype, 13.9 mm SL.

**Table 1.** Morphometric data of *Trichomycterus saquarema* Costa, Katz, Vilaro and Amorim sp. nov.

	Holotype	Paratypes (n = 6)
Standard length (SL)	53.1	45.8–56.7
<b>Percentage of standard length</b>		
Body depth	13.3	12.0–14.3
Caudal peduncle depth	11.3	9.1–11.6
Body width	11.2	9.5–11.7
Caudal peduncle width	3.2	2.9–5.4
Pre-dorsal length	61.9	60.0–65.4
Pre-pelvic length	57.9	55.9–58.6
Dorsal-fin base length	12.6	10.4–11.8
Anal-fin base length	10.0	8.4–10.6
Caudal-fin length	15.9	15.0–17.0
Pectoral-fin length	14.4	12.7–13.8
Pelvic-fin length	10.7	9.6–11.1
Head length	20.8	20.3–21.3
<b>Percentage of head length</b>		
Head depth	46.5	43.3–47.9
Head width	87.0	83.4–90.2
Snout length	40.8	38.7–40.1
Interorbital width	29.6	28.7–31.0
Preorbital length	11.0	10.1–12.0
Eye diameter	10.9	11.0–13.5

**Diagnosis.** *Trichomycterus saquarema* is a member of the *T. purioventris* complex, in which specimens above about 30 mm SL have a colour pattern consisting of a longitudinal row of dark brown to black spots along the longitudinal flank midline, with spots frequently united by melanophores to form a longitudinal stripe, whereas distinctive spots are absent below the longitudinal midline (vs. never a similar colour pattern). *Trichomycterus saquarema* is distinguished from *T. purioventris*, the only other species of the *T. purioventris* complex by having fewer procurent caudal-fin rays (13–15 dorsal and 11 ventral procurent caudal-fin rays, vs. 17–19 and 13–16, respectively; a shorter nasal barbel, its tip posteriorly reaching the area between the orbit and the opercle (vs. reaching the opercular patch of odontodes); a shorter maxillary barbel, its tip posteriorly reaching between the anterior and middle portions of the interopercular patch of odontodes (vs. reaching the area between the interopercle and the pectoral-fin base); a shorter pectoral-fin filament, its length about 20 % or less of the pectoral-fin length (vs. about 40 %); and a narrower autopalatine, autopalatine largest width smaller than autopalatine osseous length, excluding postero-lateral process (Figure 2D; vs. larger, Figure 2C). *Trichomycterus saquarema* is also distinguished from all other species of *Psammocambeva* from RPSA by the presence of bluish silver spots on the dorsum in live specimens between about 30 and 50 mm SL (vs. absence of bluish silver spots) and urogenital papilla situated at a vertical through the dorsal-fin origin, or slightly anterior to it (vs. posterior to a vertical through the dorsal-fin origin).

**Description.** General morphology: Morphometric data appear in Table 1. Body moderately slender, subcylindrical, slightly depressed anteriorly, compressed posteriorly. Greatest body depth at vertical immediately anterior to pelvic-fin base. Dorsal and ventral profiles of the head and trunk are slightly convex, about straight on the caudal peduncle. Anus and urogenital papilla at vertical through the dorsal-fin origin. Head sub-trapezoidal in dorsal view. The anterior profile of the snout is slightly convex in the dorsal view. Eye relatively small, dorsally positioned in the head, nearer snout tip than the posterior border of opercle. Posterior nostril nearer anterior nostril than orbit. Tip of nasal barbel posteriorly reaching area between orbit and opercle; the tip of maxillary and rictal barbels posteriorly reaching between anterior and middle portions of interopercular patch of odontodes. Mouth subterminal. Jaw teeth 45–51 in the premaxilla, 60–63 in the dentary; teeth irregularly arranged, pointed. Opercular odontodes 14–16, interopercular odontodes 38–46. Ventral surface of head with minute papillae.

The dorsal and anal fins are subtriangular, and the distal margin is weakly convex. Total dorsal-fin rays 11 (ii + II + 7), total anal-fin rays 9 (ii + II + 5). Anal-fin origin at vertical through the posterior portion of dorsal-fin base, between the 5th and 6th branched rays. The pectoral fin is subtriangular in dorsal view, the posterior margin slightly convex, and the first pectoral-fin ray terminating in filament reaching about 20% or less of pectoral-fin length. The total pectoral-fin rays are 7 or 8 (I + 6–7). The posterior extremity of the pelvic fin truncates, at the vertical through the anterior half of the dorsal-fin base and posterior to urogenital aperture. Pelvic-fin bases are medially separated by interspace about one-third of the fin base width. Total pelvic-fin rays 5 (I + 4). Caudal fin subtruncate, posterior corners rounded. Total principal caudal-fin rays 13 (I + 11 + I), total dorsal procurent rays 13–15 (xii–xiv + I), total ventral procurent rays 11 (x + I). Vertebrae 37. Ribs 11–13.

Laterosensory system: Supraorbital, posterior section of infraorbital, and postorbital sensory canals continuous. Supraorbital pores 3, all paired: s1, adjacent to the medial margin of anterior nostril; s3, adjacent and just posterior to the medial margin of posterior nostril; s6, at the transverse line through posterior margin of orbit. Pores s6 is slightly nearer to its homologous pair than orbit. The infraorbital sensory canal is arranged in 2 segments; the anterior section is isolated, with two pores: i1, at the transverse line through the anterior nostril, i3, at the transverse line just anterior to posterior nostril; the posterior segment posteriorly connected to supraorbital and postorbital canal, with 2 pores: i10, adjacent to the ventral margin of the orbit, i11, posterior to orbit. Postorbital canal with 2 pores: po1, at the vertical line above the posterior portion of the interopercular patch of odontodes, po2, at the vertical line above the posterior portion of the opercular patch of odontodes. The lateral line of the body is short, with 2 pores just posterior to the head.

Colouration in life (Figure 14): Larger adult specimens above about 50 mm SL: flank and dorsum light brownish yellow, with three longitudinal rows of round black spots, one along the dorsum midline, one along the flank midline, and one on the dorsal part of flank; black rows frequently united by melanophores to form longitudinal stripe. Melanophores are concentrated on the flank area just posterior and above the pectoral-fin base for black humeral blotch. No distinctive black spots on the zone below the lateral midline posterior to humeral blotch, but melanophores are weakly dispersed on the ventral portion of the caudal peduncle. Venter yellowish white. The headlight is brownish yellow, with superficial melanophores scattered over lateral and dorsal surfaces, more concentrated above the opercle and interopercle and between nares; orangish yellow pigmentation concentrated around the orbit, snout, and below opercle; transverse series of short black lines on a postero-ventral portion of interopercle. The barbel's are grey, and nasal barbels are darker. Iris bluish silver. Fins hyaline with dark yellow bases impregnated with superficial melanophores. Specimens between about 30 and 50 mm SL: similar to larger specimens, except for the presence of rows of bluish silver spots alternated with black spots. Juvenile specimens between about 15 and 30 mm SL: flank and dorsum light grey, with three black stripes, one along the dorsum midline, one along the flank midline, and one on the dorsal part of the flank. Venter white. The lateral and ventral portions of the head are light grey, the dorsal portion is black. Nasal barbel dark grey, maxillary, and rictal barbels white. Iris bluish silver. Fins hyaline.

Colouration in alcohol: Similar to colouration in live specimens, except for the absence of bright colours.

*Etymology.* The name *saquarema* refers to the occurrence of the new species in the Lagoa de Saquarema system. The word *saquarema* is derived from the Tupi-Guarani, but its meaning is not clear.

*Distribution and habitat notes.* *Trichomycterus saquarema* is presently known from a single locality in the Rio Roncador, a tributary of Lagoa de Saquarema, at about 90 m asl (Figure 5). The type locality is a fast-flowing stream, about 4 m wide and 1 m deep in deeper areas, with clear water, and the bottom comprised of sand and gravel substrate in shallower places and leaf litter and mud in deeper areas, with zones with stones to about 1 m in diameter (Figure 15A). Smaller specimens of *T. saquarema* were found over sand and gravel



substrate, whereas the few larger specimens were found buried in the muddy substrate. The area is situated in a mosaic of original forest remnants and lands used for agricultural purposes.

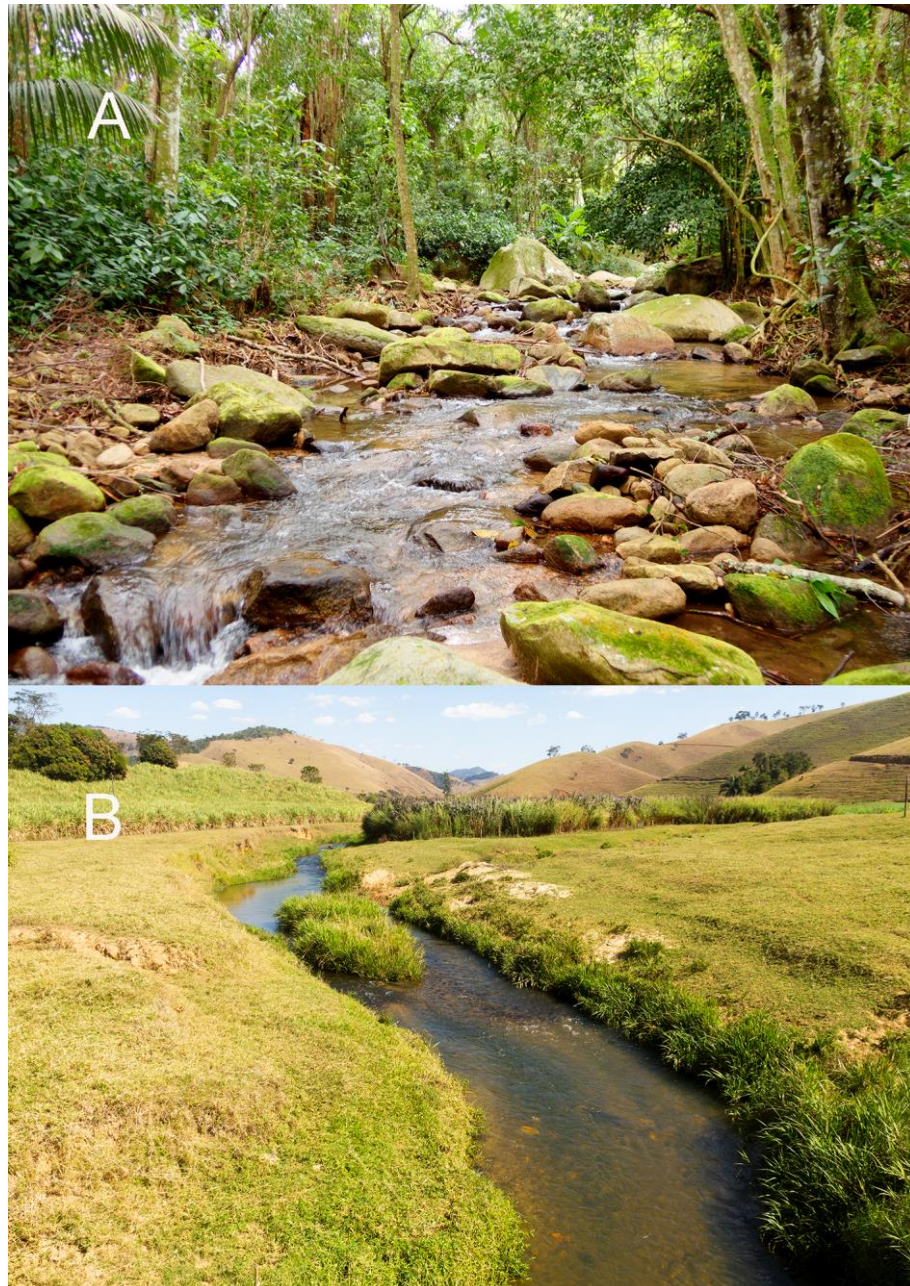


**Figure 15.** Type localities of (A) *Trichomycterus saquarema* Costa, Katz, Vilardo and Amorim, sp. nov.; (B) *Trichomycterus altipombensis* Costa, Katz, Vilardo and Mattos, sp. nov.

Freshwater fishes of this system were inventoried in 1982 by one of us [46], but field collections were then limited to the lowest areas, and no trichomycterids were found. Therefore, *T. saquarema* is the first record of a trichomycterid catfish for the Lagoa de Saquarema system.

### 3.5. The *Trichomycterus travassosi* Complex

This complex comprises three species: *T. macrophthalmus* (Figure 16), *T. travassosi* (Figure 17), and a new species below described (Figure 18). All three are endemic to the Rio Paraíba do Sul basin, occurring in disjunct areas between about 300 and 600 m asl:

*T. macrophthalmus*, from the upper Rio Pirai drainage, middle Rio Paraíba do Sul basin; *T. travassosi*, from tributaries of the upper Rio Paraíba do Sul basin, and the new species, from the upper Rio Pomba drainage, lower Rio Paraíba do Sul basin (Figure 5). Species of this clade differ from other congeners of PAC by having more dorsal procurrent caudal-fin rays (22–28 vs. 15–19) and a laminar expansion on the dorsal surface of the autopalatine articulation for the lateral ethmoid, slightly projecting over the latter bone (Figure 2E,F).



**Figure 16.** *Trichomycterus macrophthalmus*, UFRJ 5683, paratype, 56.2 mm SL: (A) lateral, (B) dorsal, and (C) ventral views.



**Figure 17.** *Trichomycterus travassosi*, UFRJ 5190, 57.2 mm SL: (A) lateral, (B) dorsal, and (C) ventral views.

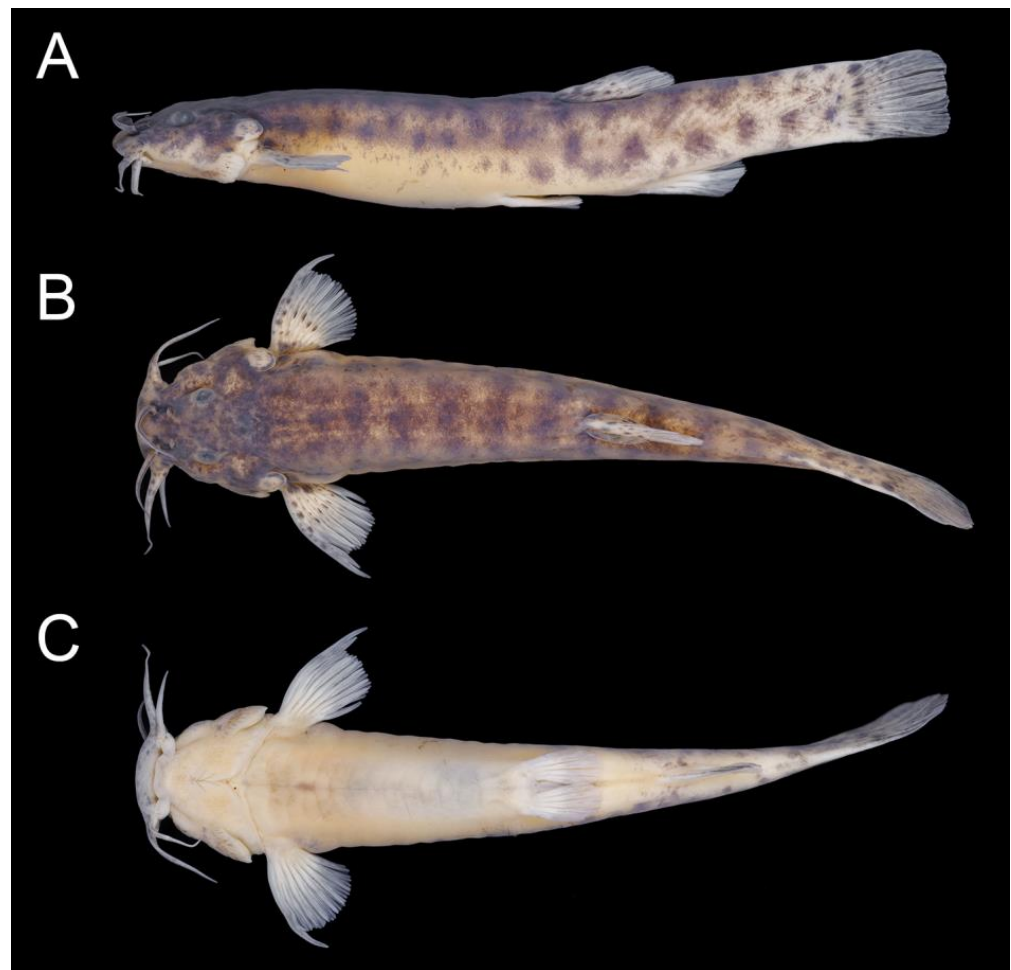


**Figure 18.** *Trichomycterus altipombensis* Costa, Katz, Vilaro and Mattos, sp. nov., UFRJ 13211, holotype, 53.5 mm SL: (A) lateral, (B) dorsal, and (C) ventral views.

All these three species also share a colour pattern that is not present in other congeners from RPSA, comprising a longitudinal row of dark brown to black round spots, posteriorly ending in spots slightly ventrally displaced, making the spots centre below the lateral midline of the body (Figures 16–18), thus differing from other spotted congeners, in which posterior spots centres are nearly coincident with the lateral body midline (Figures 5–7, 12 and 13). Among congeners, a similar colour pattern is also present in *Trichomycterus mimosensis* Barbosa, 2013, but this species does not share the two apomorphic conditions above described for this species complex (i.e., 17 or 18 dorsal procurrent caudal-fin rays and no laminar expansion on the dorsal surface of the autopalatine articulation), and its phylogenetic position is still uncertain since molecular data were not available for topotypes. The sister species *T. travassosi* and *T. macrophthalmus* share the presence of a prominent dorsal membranous expansion on the caudal peduncle, forming a distinctive keel (Figures 16 and 17; vs. dorsal membranous expansion rudimentary or absent). See the diagnosis for the new species and key for identification below for a complete list of morphological characters useful to distinguish species of the *T. travassosi* complex.

*Trichomycterus altipombensis* Costa, Katz, Vilaro and Mattos, sp. nov.

LSID:urn:lsid:zoobank.org:act:B05B2046-D949-4272-8EC4-0BD82A1DB3BE.

Figures 18 and 19, Table 2.

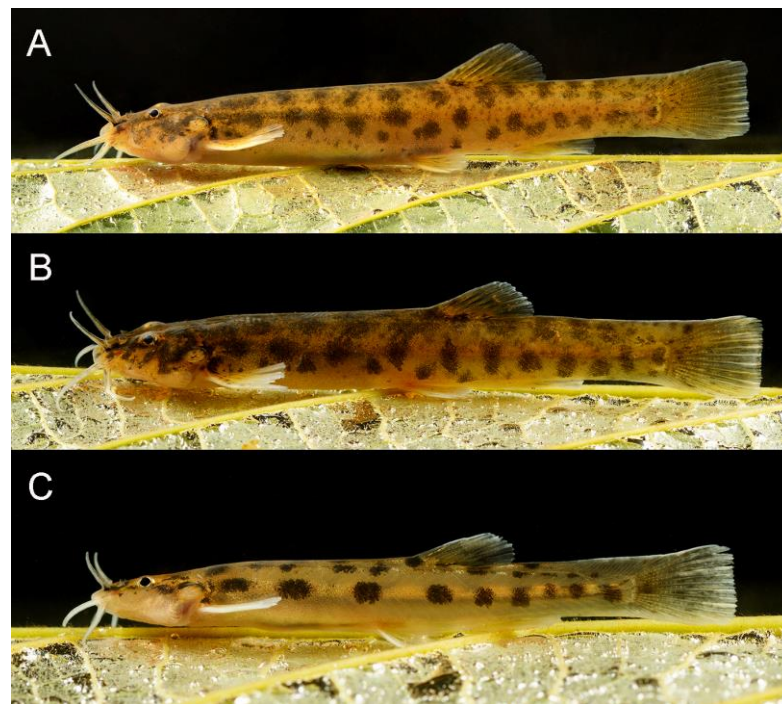


**Figure 19.** Live specimens of *Trichomycterus altipombensis* Costa, Katz, Vilaro and Mattos, sp. nov. (A) UFRJ 12784, paratype, 59.0 mm SL; (B) UFRJ 12784, paratype, 43.0 mm SL; (C) UFRJ 12784, paratype, 34.0 mm SL.

**Table 2.** Morphometric data of *Trichomycterus altipombensis* Costa, Katz, Vilaro and Mattos sp. nov.

	Holotype	Paratypes ( $n = 10$ )
Standard length (SL)	53.5	44.3–70.8
<b>Percentage of standard length</b>		
Body depth	14.9	14.7–15.7
Caudal peduncle depth	11.5	10.5–12.5
Body width	13.2	11.7–14.5
Caudal peduncle width	4.1	3.3–4.6
Pre-dorsal length	60.4	56.6–62.6
Pre-pelvic length	54.8	51.3–57.1
Dorsal-fin base length	9.7	11.8–13.0
Anal-fin base length	8.4	7.3–9.7
Caudal-fin length	16.7	14.9–18.0
Pectoral-fin length	14.3	13.3–15.8
Pelvic-fin length	11.4	10.4–12.4
Head length	22.2	20.2–23.7
<b>Percentage of head length</b>		
Head depth	43.6	42.7–50.6
Head width	87.2	82.0–90.8
Snout length	46.1	41.4–49.0
Interorbital width	26.5	23.5–27.5
Preorbital length	14.2	12.5–16.8
Eye diameter	14.9	14.5–16.5

*Holotype.* UFRJ 13211, 53.5 mm SL; Brazil: Minas Gerais State: Santa Bárbara do Tigúrio Municipality: upper Rio Pomba, Rio Paraíba do Sul basin, 21°14'06" S 43°30'51" W, about 600 m asl; A. M. Katz & P. J. Vilaro, 17 July 2021.

*Paratypes.* UFRJ 12784, 23 ex., 20.9–55.9 mm SL; UFRJ 13210, 3 ex. (C&S), 38.7–42.0 mm SL; UFRJ 12770, 5 ex. (DNA), 19.9–29.1 mm SL; CICC AA 07154, 4 ex., 35.4–58.7 mm SL; collected with holotype. UFRJ 10283, 15 ex., 26.6–70.8 mm SL; UFRJ 12475, 2 ex. (C&S),

54.2–57.4 mm SL; UFRJ 10264, 3 ex. (DNA), 25.1–29.3 mm SL; same locality as holotype; M.A. Barbosa et al., 19 November 2014.

**Diagnosis.** *Trichomycterus altipombensis* is a member of the *T. travassosi* complex, differing from other species of PAC by having numerous dorsal procurrent caudal-fin rays (22–25 vs. 13–19). *Trichomycterus altipombensis* differs from the other two species of the *T. travassosi* complex, *T. macrophthalmus* and *T. travassosi*, by the absence of a prominent dorsal membranous expansion on the caudal peduncle, forming a distinctive keel (vs. presence); by having the anal-fin origin posterior to the dorsal-fin base (vs. anal-fin origin at a vertical through the posterior portion of the dorsal-fin base), caudal fin truncate, posterior margin straight (vs. subtruncate, posterior margin slightly rounded). *Trichomycterus altipombensis* is also distinguished from all other species of PAC from RPSA by the presence of a notch on the posterolateral margin of the premaxilla (vs. notch absent) and the metapterygoid with a curved posterior tip (vs. straight).

**Description.** General morphology: Morphometric data appear in Table 1. Body moderately slender, subcylindrical, slightly depressed anteriorly, compressed posteriorly. Greatest body depth at vertical immediately anterior to pelvic-fin base. Dorsal and ventral profiles of the head and trunk are slightly convex, about straight on the caudal peduncle. Anus and urogenital papilla at vertical just anterior to middle of the dorsal-fin base. Head subtrapezoidal in dorsal view. The anterior profile of the snout is slightly convex in the dorsal view. Eye relatively large, dorsally positioned in the head, about equidistant from snout tip and posterior border of opercle. Posterior nostril nearer anterior nostril than orbit. Tip of nasal barbel posteriorly reaching area between orbit and opercle; the tip of maxillary and rictal barbels posteriorly reaching the posterior portion of interopercular patch of odontodes or area just posterior to it. Mouth subterminal. Jaw teeth 29–39 in the premaxilla, 42–53 in the dentary; teeth irregularly arranged, pointed in the premaxilla, pointed or with rounded extremity in the dentary. Opercular odontodes 17–21, interopercular odontodes 29–39. Ventral surface of head with minute papillae.

The dorsal and anal fins are subtriangular, and the distal margin is straight. Total dorsal-fin rays 11 (ii + II + 7), total anal-fin rays 9 (ii + II + 5). Anal-fin origin at vertical immediately posterior to dorsal-fin base. Pectoral fin subtriangular in dorsal view, posterior margin convex, first pectoral-fin ray terminating in filament reaching about 20 % or less of pectoral-fin length. Total pectoral-fin rays 8 (I + 7). The posterior extremity of the pelvic fin is rounded and vertical through the middle of the dorsal-fin base and posterior to the urogenital aperture. Pelvic-fin bases are medially separated by interspace slightly shorter than half width of the fin base. Total pelvic-fin rays 5 (I + 4). Caudal fin subtruncate, posterior corners rounded. Total principal caudal-fin rays 13 (I + 11 + I), total dorsal procurrent rays 22–25 (xxi–xxiv + I), total ventral procurrent rays 12 (xi + I). Vertebrae 34–36. Ribs 10 or 11.

Laterosensory system: Supraorbital, posterior section of infraorbital, and postorbital sensory canals continuous. Supraorbital pores 3, all paired: s1, adjacent to the medial margin of anterior nostril; s3, adjacent and just posterior to the medial margin of posterior nostril; s6, at the transverse line through posterior margin of orbit. Pores s6 medially are in close proximity. The infraorbital sensory canal is arranged in 2 segments; the anterior section is isolated, with two pores: i1, at the transverse line through the anterior nostril, i3, at the transverse line just anterior to posterior nostril; the posterior segment posteriorly connected to supraorbital and postorbital canal, with 2 pores: i10, adjacent to the ventral margin of the orbit, i11, posterior to orbit. Postorbital canal with 2 pores: po1, at the vertical line above the posterior portion of the interopercular patch of odontodes, po2, at the vertical line above the posterior portion of the opercular patch of odontodes. The lateral line of the body is short, with 2 pores just posterior to the head.

Colouration in life (Figure 19): In specimens above about 30 mm SL, the flank and dorsum are light yellow, with rounded dark brown spots and minute dark grey dots irregularly arranged. Venter yellowish white. Headlight yellow, with melanophores scattered over lateral and dorsal surfaces, more concentrated above opercle and interopercle

and between nasal barbel and orbit. Nasal barbel grey, maxillary, and rictal barbels white, with minute black dots on the dorsal surface of maxillary barbel. Iris light yellow. Fins yellowish hyaline with minute black dots on the basal portion. In specimens below about 30 mm SL, body spots are black and arranged in three longitudinal rows, one along the dorsum midline, one between the anterior lateral midline and ventral portion of the caudal peduncle just anterior to caudal-fin base, and one on the dorsal part of the flank.

Colouration in alcohol: Similar to colouration in live specimens, but with paler colours.

*Etymology.* The name *altipombensis* is an allusion to the occurrence of the new species in the upper section of the Rio Pomba.

*Distribution and habitat notes.* *Trichomycterus altipombensis* is only known from the upper Rio Pomba drainage, Rio Paraíba do Sul basin, at about 600 m asl (Figure 5). At the type locality, the Ribeirão Fernandes is a fast-flowing stream, with its largest width reaching about 6 m, and deepest areas not surpassing about 1 m deep. The water is clear and slightly turbid, and the bottom comprises sand and gravel substrate, where all species were found (Figure 15B). The original forest vegetation was removed and substituted by cane plantations.

### 3.6. Key to Identification of Species of *Psammocambeva* from RPSA

1A. No spot on flank; 48–62 opercular odontodes; 92–100 interopercular odontodes; nine pectoral-fin rays; caudal fin emarginate . . . . . *T. largoperculatus*.

1B. Flank spotted, at least in its dorsal portion; 13–21 opercular odontodes; 31–57 interopercular odontodes; eight pectoral-fin rays; caudal fin subtruncate or truncate . . . . . 2.

2A. Dorsal extremity of branchiostegal membrane touching ventral margin of an opercular patch of odontodes . . . . . 3.

2B. Dorsal extremity of branchiostegal membrane touching posterior margin of an opercular patch of odontodes . . . . . 8.

3A. Lower jaw teeth incisiform; body colouration highly variable in adult specimens, polymorphic . . . . . *T. jacupiranga*.

3B. Lower jaw teeth pointed or with slightly rounded tip; body colouration with little or no conspicuous variation in adult specimens . . . . . 4.

4A. Flank midline with longitudinal row of dark brown to black spots in close proximity, with spots, frequently united by melanophores to form a longitudinal stripe; flank below midline without dark brown to black spots; eye not dorsally protruded; s6 pores always paired; dorsal procurrent caudal-fin rays 13–19 . . . . . 5.

4B. Flank midline with longitudinal row of dark brown to black spots separated by interspaces, never forming a stripe; flank below midline with dark brown to black round spots; eye slightly dorsally protruded; s6 pores usually single, rarely paired in a few specimens; dorsal procurrent caudal-fin rays 22–28 . . . . . 6.

5A. 17–19 dorsal procurrent caudal-fin rays; 13–16 ventral procurrent caudal-fin rays; the tip of nasal barbel posteriorly reaching an opercular patch of odontodes; maxillary barbel posteriorly reaching between interopercle and pectoral-fin base; pectoral-fin filament length about 40 % of pectoral-fin length . . . . . *T. purioventris*.

5B. 13–15 dorsal procurrent caudal-fin rays; 11 ventral procurrent caudal-fin rays; the tip of nasal barbel posteriorly reaching between orbit and opercle; maxillary barbel posteriorly reaching between anterior and middle portions of an interopercular patch of odontodes; pectoral-fin filament length about 20 % or less of pectoral-fin length . . . . . *T. saquarema*.

6A. Caudal peduncle without prominent dorsal membranous expansion; anal-fin origin at vertical posterior to dorsal-fin base; caudal fin truncates, posterior margin straight . . . . . *T. altipombensis*.

6B. Caudal peduncle with prominent dorsal membranous expansion, forming distinctive keel; anal-fin origin at vertical through the posterior portion of dorsal-fin base; caudal fin subtruncate, posterior margin slightly rounded . . . . . 7.

7A. Eye large, about 13–15 % of head length; nasal barbel posteriorly reaching orbit; maxillary barbel gradually narrowing distally; the longitudinal row of spots on the lateral midline of flank united to the longitudinal row of spots on the dorsolateral portion of flank to form transverse bars; 25–28 dorsal procurrent caudal-fin rays ... ..  
*T. macrophthalmus*.

7B. Eye relatively small, about 8.5–11 % of head length; nasal barbel posteriorly reaching area between orbit and opercle; maxillary barbel abruptly narrowing distally near its base; the longitudinal row of spots on the lateral midline of flank separated from the longitudinal row of spots on the dorsolateral portion of flank; 22–24 dorsal procurrent caudal-fin rays ... ..  
*T. travassosi*.

8A. Nasal barbel posteriorly reaching area just posterior to orbit; eye always larger than an opercular patch of odontodes; supraorbital canal usually interrupted, forming two separate segments; anterior portion of the lateral midline of flank with a row of brown spots deeper than long, separated by broader interspaces, never forming stripe ... ..  
*T. auroguttatus*.

8B. Nasal barbel posteriorly reaching area just anterior to opercle; eye and an opercular patch of odontodes nearly equal in specimens above about 40 mm SL; supraorbital canal always continuous; anterior portion of the lateral midline of flank with a row of brown spots longer than deep, in close proximity and often united to form stripe ... ..  
*T. goeldii*.

#### 4. Discussion

##### 4.1. *Psammocambeva* Taxonomy

During the last decades, *Trichomycterus* was considered a problematic taxon, not having an objective diagnosis based on unique characters states, consequently comprising a paraphyletic assemblage of numerous species broadly distributed in South America (see a recent historical review in [7]). A new perspective was provided with the publication of molecular phylogenies involving taxa representing the main trichomycterine lineages [1,2], which allied to a historical review about the type species of *Trichomycterus* [26] has allowed a quick advance in the genus taxonomy [7]. *Trichomycterus* was then restricted to an eastern South American clade containing the type species of the genus, the *Trichomycterus s.s.* clade [1,7]. In an attempt to make easier species placement in *Trichomycterus s.s.*, Costa [7] divided it into six subgenera based on an integrative approach, combining a multigene dataset and osteological data to establish monophyletic unities diagnosable by morphological data. In that study, no unique apomorphic feature was found to diagnose the subgenus *Psammocambeva*. However, morphological characters may be still useful to diagnose monophyletic species groups within *Psammocambeva* [13], as here described.

In a paper on the systematics of *Trichomycterus s.s.* from the Rio Doce basin, Reis & de Pinna [21] proposed to solve some supposed taxonomical problems related to species occurring in that basin using an iterative approach using DNA, phylogeny, and ‘classical taxonomy’. The phylogeny was restricted to a small segment of the mitochondrial gene cytochrome oxidase subunit I (cox1), 650 bp, and no explicit operational method for species delimitation was employed, with the authors advocating the use of diagnosability of morphological characters associated with tree topology to delimitate species. However, among the six new species described in that paper, three were based only on morphological data. Species were diagnosed by colour patterns and details of the external morphology, omitting informative osteological characters available in the literature. The resulting tree presented a low resolution for the numerous haplotypes from the Rio Doce, which did not cluster to form exclusive lineages, probably as a result of using a short segment of cox1 for a sample also including distantly related trichomycterines. However, in this context, Reis & de Pinna [21] concluded that *T. alternatus* is a meta-species, including in its synonymy nominal species that the authors did not find distinguishing morphological characters, such as *T. auroguttatus*, *T. longibarbatatus*, and *T. travassosi*. As above described and discussed,

all these three species are not the closest relatives of *T. alternatus* (Figure 1) and they can be consistently distinguished from *T. alternatus* by morphological data.

The present study corroborates *T. auroguttatus*, endemic to the upper Rio Preto drainage, Rio Paraíba do Sul basin, as a member of the *T. goeldii* complex, which also includes *T. alternatus*, *T. astromycterus*, and *T. goeldii* (Figure 1). *Trichomycterus auroguttatus* is supported as a sister to *T. goeldii*, whereas *T. alternatus* is supported as a sister to *T. astromycterus*, indicating that *T. auroguttatus* is not a synonym of *T. alternatus* as proposed by Reis & de Pinna [21]. In addition, *T. auroguttatus* differs from *T. alternatus* by some morphological character states, including characteristics of the external morphology: the presence of a shorter nasal barbel; the orbital diameter larger than the opercular patch of odontodes; supraorbital canal interrupted, forming two separate segments; and brown spots of the anterior portion of a row of spots on the longitudinal midline of flank deeper than long, separated by broader interspaces, never forming a stripe; and two osteological characters: the presence of a robust comma-shaped osseous core in the autopalatine articular shell for the lateral ethmoid, and a widened third hypobranchial, with its anterior extremity distinctively wider than the anterior extremity of the second hypobranchial (see Results above and included illustrations). Therefore, *T. auroguttatus* is not a synonym of *T. alternatus*.

*Trichomycterus longibarbatus*, placed in the synonymy of *T. alternatus* together with *T. auroguttatus* and *T. travassosi*, was first described based on specimens from Santa Teresa, Espírito Santo, south-eastern Brazil [17]. According to data provided by the holotype collector (Sérgio Potsch, person. comm., 23 June 2022), the type locality is situated within a private area (Sítio do Alcebiades), on the road to Nova Lombardia, in a small stream belonging to the upper Rio Piraquê-Açu drainage, lower Rio Doce basin. Despite *T. alternatus* and *T. longibarbatus* being endemic to the same river basin (i.e., Rio Doce basin), and having a superficially similar colour pattern (i.e., dark spots on the flank), the latter species is easily distinguished from all species of *Psammocambeva* by having longer barbels (see also results above). When comparing osteological characters, distinguishing features are still more evident. Firstly, *T. longibarbatus* does not exhibit the diagnostic features of the *T. goeldii* complex. The autopalatine and the maxilla have different morphology (Figure 2H), not showing any of the apomorphic features described for the *T. goeldii* complex. Secondly, *T. longibarbatus* differs from all other taxa of *Trichomycterus* s.s. by having an axe-like interopercular dorsal process (Figure 4B) and an approximately straight premaxilla (Figure 2H). Finally, *T. longibarbatus* is supported as a sister to the whole PAC (Figure 1). Therefore, *T. longibarbatus* is not a synonym of *T. alternatus*.

*Trichomycterus travassosi* does not have any of the osteological diagnostic features of the *T. goeldii* complex (see above), which is evidence that *T. travassosi* is not a synonym of *T. alternatus*. In *T. travassosi*, the medial margin of the autopalatine is almost straight, the postero-lateral process is short, and the maxilla is nearly straight (Figure 2E). Externally, the general color pattern, the fin morphology, and the latero-sensory system do not provide characters useful to non trichomycterine experts, easily distinguishing *T. travassosi* from *T. alternatus*, but some details of the head and caudal peduncle morphology make possible to readily distinguish these species: in *T. travassosi* the maxillary barbel abruptly narrows in its sub proximal portion (Figure 17B; vs. gradually narrowing in *T. alternatus*, Figure 7B); the branchiostegal membrane dorsally reaches the ventral margin of the opercular patch of odontodes (Figure 17A; vs. reaching the posterior margin of the opercular patch of odontodes in *T. alternatus*, Figure 7A); the lateral fleshy lobes of the mouth are conspicuously thickened (Figure 17C; vs. not thickened in *T. alternatus*, Figure 7C), and there is a prominent dorsal membranous expansion on the caudal peduncle, forming a distinctive keel (Figure 17A; no prominent expansion in *T. alternatus*, Figure 7A). Therefore, *T. travassosi* cannot be considered as a synonym of *T. alternatus*.

The species here identified as *Trichomycterus jacupiranga* was identified by Reis & de Pinna [20,21] as *T. alternatus*, which was followed by Donin et al. [47], whereas Lima et al. [48] identified it as *T. aff. alternatus*. *Trichomycterus jacupiranga* was described based on specimens collected in the Rio Ribeira de Iguape basin [49], but our recent molecular and



morphological studies indicate that *T. jacupiranga* is geographically widespread along the coastal basins of south-eastern Brazil, with high levels of colouration polymorphism (Vilardo et al., unpublished). In the RPSA, *T. jacupiranga* occurs in most coastal basins between the rivers connected to the Baía de Guanabara and those connected to the Baía da Ilha Grande, whereas populations exhibiting similar morphology but with taxonomical status still undetermined (herein identified as *T. cf. jacupiranga*) are found in eastern coastal basins (Figure 5). As above described, no morphological synapomorphy diagnosing the *T. goeldii* complex is found in *T. jacupiranga*, which does not support *T. jacupiranga* as being conspecific with *T. alternatus* and other species of the *T. goeldii* complex. In *T. jacupiranga* (Figure 2G), the medial margin of the autopalatine is weakly sinuous, not exhibiting a deep concavity and the postero-lateral autopalatine process is not long as in species of the *T. goeldii* complex (Figure 2A,B), as well as the premaxilla is only slightly curved (Figure 2G), not showing the peculiar morphology recorded for species of the *T. goeldii* complex (Figure 2A,B). *Trichomycterus jacupiranga* exhibits high colouration polymorphism, thus not being possible to clearly distinguish it from species of the *T. goeldii* complex by colour patterns only, but *T. jacupiranga* is easily distinguished by having incisor-like teeth in the dentary, instead of pointed to slightly rounded as in *T. alternatus* and other species of the *T. goeldii* complex. In addition, the molecular phylogenetic analyses indicate that *T. jacupiranga* is not closely related to species of the *T. goeldii* complex (Figure 1).

#### 4.2. Perils of Underestimating Species Diversity

The region where the RPSA is situated is among the most populous in South America, with the original forest being gradually lost since the 16th century and today restricted to small, isolated fragments. During over five centuries, numerous economic activities have contributed to an intense and increasing environmental degradation, including agropastoral activities, industries, and tourism, in addition to a strong urbanization process, resulting in large cities and important tourist complexes [50]. Despite national parks and other biological reserves protecting headwater areas, the entire hydrographic network is highly affected by pollution and dams, causing a large part of the ichthyofauna to be threatened with extinction [51,52]. Therefore, species diversity estimates in taxonomic revisions are primary tools of great importance [53], being constantly used to assess the conservation status of local species.

Following the results of Reis & de Pinna [21], where *T. auroguttatus* and *T. travassosi* are considered synonyms of *T. alternatus*, *T. purioventris* is suggested to be a synonym of *T. alternatus*, the species from the coastal basins (here identified as *T. jacupiranga*) is identified as *T. alternatus*, the taxonomic status of *T. goeldii* is not assessed, and *T. macrophthalmus* is omitted, technicians from environmental agencies would possibly identify all species of PAC from RPSA as belonging to a single species, *T. alternatus*. This supposed widespread species, with a wide distribution in the basins of south-eastern Brazil, would be then considered a species of least concern for conservation strategies, which would have a catastrophic effect on the conservation of species that occur in restricted, unprotected areas, and under the strong environmental impact, such as *T. altipombensis*, *T. macrophthalmus*, *T. purioventris*, and *T. saquarema*. Thus, without recognition of their taxonomic status and consequently without specific policies for their conservation, these species would then be doomed to disappear in the near future.

Other negative consequences could also be considered if different species of PAC from RPSA were mistakenly identified as a single species. In this case, studies on reproduction, ecology, and behaviour could generate highly conflicting and unexplainable data since some of these species have different biological characteristics. For example, comparing *T. auroguttatus* and *T. travassosi* that live in nearby areas (Figure 5) and were both explicitly considered synonyms of *T. alternatus* by Reis & de Pinna [21], our field observations indicate that the first species occurs at altitudes between about 1000 and 1200 m asl and has sand-bearing habits, whereas the second occurs at altitudes between about 400 and 600 m asl, being more generalist, found both in sand and gravel substrate [7,17]. Therefore, it would

be plausible to find divergent ecological characteristics for these species following our field data and structural morphological differences (see osteological characters above described), but incorrect identification would cause great harm to the correct interpretation of data.

## 5. Conclusions

Taxonomic reviews using integrative approaches are important tools to estimate species diversity, especially in areas under the intense process of environmental decline, such as mountainous areas of south-eastern Brazil [53]. However, as discussed here, these approaches must necessarily include a range of morphological characters that are informative to delineate and diagnose groups and their respective species in association with phylogenies generated by robust molecular datasets.

**Author Contributions:** Conceptualization, W.J.E.M.C.; data obtaining, W.J.E.M.C., J.L.M., P.J.V., P.F.A. and A.M.K.; formal analysis, W.J.E.M.C. and J.L.M.; investigation, W.J.E.M.C., P.J.V. and A.M.K.; data curation, W.J.E.M.C., J.L.M., P.J.V., P.F.A. and A.M.K.; writing—original draft preparation, W.J.E.M.C.; visualization, W.J.E.M.C., J.L.M. and A.M.K.; supervision, W.J.E.M.C.; project administration, W.J.E.M.C.; funding acquisition, W.J.E.M.C., J.L.M., P.J.V. and A.M.K. All authors have read and agreed to the published version of the manuscript.

**Funding:** This study was supported by Conselho Nacional de Desenvolvimento Científico e Tecnológico (CNPq; grant 304755/2020-6 to WJEMC and 140689/2022-2 to PJV), Fundação Carlos Chagas Filho de Amparo à Pesquisa do Estado do Rio de Janeiro (FAPERJ; grant E-26/201.213/2021 to WJEMC, 202.327/2018 and 202.328/2018 to JLOM; and E-26/202.005/2020 to AMK), and Coordenação de Aperfeiçoamento de Pessoal de Nível Superior (CAPES; grant 88887.466724/2019-00 to PFA). This study was also supported by CAPES (Coordenação de Aperfeiçoamento de Pessoal de Nível Superior, Finance Code 001) through the Programa de Pós-Graduação em: Biodiversidade e Biologia Evolutiva/UFRJ and Genética/UFRJ.

**Institutional Review Board Statement:** The animal study protocol was approved by the Ethics Committee for Animal Use of Federal University of Rio de Janeiro (protocol code: 065/18, approved on August 2018).

**Informed Consent Statement:** Not applicable.

**Data Availability Statement:** DNA sequences used in this study are deposited in GenBank.

**Acknowledgments:** Thanks are due to Claudia Bove, Bruno Costa, Anais Barbosa, Beatriz Oliveira and Orlando Conceição for helping in collecting trips; to James Maclaine for kindly providing photographs and radiographs of the type specimens of *T. goeldii*; to Kevin Swagel for sending photographs and radiographs of type specimens deposited in the Field Museum of Natural History; to Décio Moraes Jr. for hospitality and providing access to examine type specimens deposited in Museu Nacional; to Julia Krusemark and Thalita Seidling for help during collecting trips; to Sâmela Lopes and Luiza Petitinga for technical assistance; and to Giulia Aranha for support during DNA sequencing process.

**Conflicts of Interest:** The authors declare no conflict of interest. The funders had no role in the design of the study; in the collection, analyses, or interpretation of data; in the writing of the manuscript; or in the decision to publish the results.

## Appendix A

List of material examined of *Trichomycterus (Psammocambeva)*. All localities in Brazil. Species name is followed by catalog number, number of specimens, river basin, municipality, state (BA, Bahia; ES: Espírito Santo; MG: Minas Gerais; RJ: Rio de Janeiro; SP: São Paulo), coordinates. C&S, specimens cleared and stained for osteology; H, holotype; P, paratypes; S, syntype.

*Trichomycterus alternatus* (Eigenmann 1917): FMNH 58082, H, FMNH 58083, 62 p (photographs and radiographs); UFRJ 0080, 9, UFRJ 0080, 1 (C&S), UFRJ 0556, 2 (C&S), UFRJ 0836, 2, Rio Doce basin, Ipatinga, MG, 19°28' S 42°33' W; UFRJ 9900, 25, Rio Doce basin, Timóteo, MG, 19°38' S 42°37' W. *Trichomycterus astromycterus* Reis, de Pinna &

**Pessali 2019:** UFRJ 12788, 5, Rio Doce basin, Santo Antônio do Jacinto, MG, 16°32' S 40°15' W; UFRJ 13230, 2 (C&S); Rio Doce basin, Rio Doce, MG, 20°11'43" S 42°51'17" W. ***Trichomycterus auroguttatus* Costa, 1992:** MZUSP 43341, H, MZUSP 43342, 4P, UFRJ 0640, 2P, UFRJ 610, 3, UFRJ 1302, 2, UFRJ 3365, 1; UFRJ 4556, 3 (C&S); UFRJ 10478, 3, Rio Preto drainage, Resende, RJ, 22°20'03" S 44°32'29" W; UFRJ 11675, 15; Rio Preto, Resende, RJ, 22°19'45" S 44°32'19" W; UFRJ 10684, 6, Rio Preto, Resende, 22°19'06" S 44°31'16" W; UFRJ 12023, 8; Rio Preto drainage, Itatiaia, RJ, 22°18'58" S 44°35'28" W; UFRJ 12062, 4; Rio Preto, Itatiaia, RJ, 22°19'33" S 44°33'11" W; UFRJ 1637, 1, Rio Preto, Bocaina de Minas, MG, 22°19' S 44°35' W; UFRJ 10487, 5; UFRJ 11845, 1, Bocaina de Minas, MG, 22°19'27" S 44°34'57" W; UFRJ 4101, 7, UFRJ 4558, 2 (C&S), UFRJ 11673, 6, Bocaina de Minas, MG, 22°17'36" S 44°33'39" W; UFRJ 11669, 7, Bocaina de Minas, MG, 22°17'36" S 44°33'40" W. ***Trichomycterus barrocos* Reis & de Pinna, 2022:** UFRJ 13248, 1 (C&S); UFRJ 13249, 1; Rio Doce basin, Afonso Claudio, ES, 20°10'57" S 41°04'50" W. ***Trichomycterus brucutu* Reis & de Pinna, 2022:** UFRJ 13125, 1; UFRJ 13133, 1 (C&S); Rio Doce basin, Itambé do Mato Dentro, MG, 19°25' S 43°20' W. ***Trichomycterus caudofasciatus* Alencar & Costa, 2004:** UFRJ 6002, H, UFRJ 5655, 10 P, UFRJ 5656, 5 P (C&S), Alto Caparaó, Rio Itabapoana basin, MG, 20°25'54" S 41°51'57" W. ***Trichomycterus gasparinii* Barbosa, 2013:** UFRJ 8157, P, UFRJ 7542, 13 P, UFRJ 8158, 7 P (C&S), UFRJ 7543, 2 P, UFRJ 8184, 1 P (C&S), Rio Reis Magos basin, Fundão, ES, 19°54'60" S 40°27'86" W. ***Trichomycterus goeldii* Boulenger, 1896:** BMNH 1896.7.4-8, 2 S (photographs and radiographs), Rio Paquequer drainage, Teresópolis, RJ; UFRJ 3245, 2, UFRJ 4446, 1 (C&S), UFRJ 7874, 10, UFRJ 7880, 1, UFRJ 8242, 1, Rio Piabanha basin, Petrópolis, RJ, 22°21'22" S 43°03'35" W; UFRJ 7849, 21, Rio Piabanha basin, Petrópolis, RJ, 22°20'53" S 43°05'39" W; UFRJ 13215, 6, Rio Piabanha basin, Petrópolis, RJ, 22°20'02" S 43°11'13" W; UFRJ 4559, 1 (C&S), UFRJ 4561, 1 (C&S), Rio Piabanha basin, Petrópolis, RJ, 22°23' S 43°13' W; UFRJ 1063, 3, UFRJ 1148, 2, UFRJ 9434, 1, Rio Paquequer drainage, Teresópolis, RJ, 22°26'51" S 42°57'6" W; UFRJ 1114, 1ex, Rio Paquequer drainage, Teresópolis, RJ, 22°27'19" S 42°57'38" W; UFRJ 1121, 1, UFRJ 1123, 1, Rio Paquequer drainage, Teresópolis, RJ, 22°26'47" S 42°59'17" W; UFRJ 1064, 1, Rio Paquequer drainage, Teresópolis, RJ, 22°26'52" S 42°57'5" W; UFRJ 0263, 8, Rio Paquequer drainage, Teresópolis, RJ, 22°20' S 42°51' W; UFRJ 3386, 10, UFRJ 3387, 6, UFRJ 4448, 1 (C&S), UFRJ 4560, 2 (C&S), UFRJ 6078, 2, UFRJ 6113, 1, UFRJ 7271, 1, UFRJ 7705, 9, UFRJ 7706, 8, UFRJ 7708, 16, UFRJ 7717, UFRJ 7759, 2, 8, UFRJ 7760, 1, UFRJ 7803, 1, Rio Paquequer basin, Teresópolis, RJ, 22°25' S 42°58' W; UFRJ 7847, 3, UFRJ 7879, 6, Rio Paquequer basin, Teresópolis, RJ, 22°18'54" S 43°00'15" W; UFRJ 7938, 8, Rio Paquequer basin, Teresópolis, RJ, 22°18'54" S 43° 0'18" W; UFRJ 12468, 6, UFRJ 12668, 2 (C&S), Rio Paquequer basin, Teresópolis, RJ, 22°26'51" S 42° 59'02" W; UFRJ 12734, 1, Rio Paquequer basin, Teresópolis, RJ, 22°24'34.2" S 42°52'30.2" W; UFRJ 0721, 9, UFRJ 4562, 3 (C&S), UFRJ 5465, 6, Rio Preto basin, Valença, RJ, 22°15' S 43°56' W; UFRJ 11785, 1, Rio Preto basin, Valença, RJ, 22°17'30" S 43°54'48" W; UFRJ 11786, 20, Rio Preto basin, Conservatória, Valença, RJ, 22°16'25" S 43°56'51" W. ***Trichomycterus illuioies* Reis & de Pinna, 2022:** UFRJ 13125, 1, UFRJ 13126, 2 (C&S), Rio Doce basin, Conceição do Mato Dentro, MG, 19°01' S 43°29' S. ***Trichomycterus 'immaculatus'* (Eigenmann & Eigenmann, 1889, sense Reis & de Pinna [21]):** UFRJ 13128, 2, Rio Doce basin, Santo Antônio do Imbé, MG, 18°28' S 43°18' W; UFRJ 557, 1 (C&S), UFRJ 0082, 2, UFRJ 422, 1, UFRJ 429, 2, UFRJ 420, 6, UFRJ 557, 3 (C&S), Rio Doce basin, Ipatinga, MG, 19°30'16" S 42°34'50" W; UFRJ 11109, 3, UFRJ 10921, 3 (C&S), Rio Mucuri basin, Mucuri, BA, 18°04'45" S 39°54'54" W; UFRJ 7734, 1, UFRJ 7732, 4, UFRJ 7733, 1, Rio São Mateus basin, Nova Venécia, ES, 18°42'27" S 40°24'34" W; UFRJ 8208, 59, Rio São Mateus basin, Teófilo Otoni, MG; UFRJ 6053, 4, Rio Doce basin, Colatina, ES, 19°33'58" S 40°37'59" W; UFRJ 13234, 1, Rio Doce basin, Rio Doce, MG, 20°11'46" S 42°51'14" W; UFRJ 12789, 4, Rio Doce basin, Santo Antônio do Jacinto, MG, 16°32' S 40°15' W. ***Trichomycterus ipatinga* Reis & de Pinna, 2022:** UFRJ 13127, 2; UFRJ 13244, 2 (C&S); Rio Doce basin, Serro, MG, 18°39' S 43°27' S. ***Trichomycterus jacupiranga* Wosiacki & Oyakawa, 2005:** UFRJ 8207, 12, UFRJ 12996, 24, Rio Grande basin, Rio de Janeiro, RJ 22°56' S 43°26' W; UFRJ 8478, 35; UFRJ 8479, 20; UFRJ 8480, 8, Rio Mato Grosso, Duque de

Caxias, RJ, 22°41' S 43°16' W; UFRJ 8621, 1, Rio Estrela basin, Duque de Caxias, RJ, 22°41' S 43°16' W; UFRJ 8490, 12, Rio Santo Antônio, Duque de Caxias, RJ, 22°41' S 43°16' W; UFRJ 8475, 28, UFRJ 8476, 7, Rio do Registro, Duque de Caxias, RJ, RJ, 22°41' S 43°16' W; UFRJ 11504, 6, Rio Itaguaí basin, Itaguaí, RJ; 22°51' S 43°50' W; UFRJ 10104, 3, Rio Batatal, Mangaratiba, RJ, 22°56' S 44°02' W; UFRJ 7621, 1, Rio Bracuê, Angra dos Reis, RJ, 23°00' S 44°19' W; UFRJ 2149, 1, UFRJ 5701, 4, UFRJ 6039, 1, UFRJ 9679, 1, Rio da Guarda basin, Angra dos Reis, RJ, 23°00' S 44°19' W; UFRJ 3973, 2, UFRJ 7610, 2, Rio Mambucaba basin, Angra dos Reis, RJ, 23°01'26" S 44°30'55" W; UFRJ 1126, 8, UFRJ 1129, 9, UFRJ 1140, 6, UFRJ 4551, 2 (C&S), UFRJ 5706, 2 (C&S), Rio dos Macacos basin, Rio de Janeiro, RJ, 22°57'26" S 43°16'52" W; UFRJ 4447, 1 (C&S), UFRJ 528, 6, UFRJ 612, 5, UFRJ 1113, 1, UFRJ 1115, 2, UFRJ 1116, 2, UFRJ 1127, 3, UFRJ 1130, 3, UFRJ 1133, 3, UFRJ 1134, 4, UFRJ 1137, 10, UFRJ 1138, 6, UFRJ 1934, 8, UFRJ 3822, 13, UFRJ 4548, 1 (C&S), UFRJ 5705, 2, UFRJ 12780, 5, UFRJ 12781, 12, UFRJ 12782, 6, UFRJ 12779, 3, Rio Cascatinha basin, Rio de Janeiro, RJ, 22°57'26" S 43°16'52" W; UFRJ 12783, 22, Rio do Moke basin, Rio de Janeiro, RJ, 22°58'12" S 43°16'8" W; UFRJ 12593, 3 ex (C&S), Rio Soberbo basin, Guapimirim, RJ, 22°29'29" S 43° 0'16" W; UFRJ 8470, 17 ex; UFRJ 8471, 7 ex; UFRJ 8472, 7 ex, UFRJ 8481, 32 ex, UFRJ 8484, 8 ex; UFRJ 8485, 2 ex, UFRJ 8814, 4 ex, UFRJ 11540, 1 ex, Rio Magé basin, Magé, RJ, 22°33'20" S 43°02'57" W; UFRJ 12709, 7 ex, Rio Macaé basin, Macaé, RJ, 22°19'41" S 42°11'6" W; UFRJ 8430, 7 ex, UFRJ 8431, 1 ex, UFRJ 8477, 9 ex, UFRJ 8486, 11 ex, UFRJ 8487, 5 ex; UFRJ 8488, 7 ex, UFRJ 8489, 177 ex, UFRJ 8596, 6 ex (C&S), UFRJ 8619, 4 ex, UFRJ 8620, 13 ex, Rio Iguaçu basin, Nova Iguaçu, RJ, 22°36'58" S 43°25'52" W; UFRJ 8491, 22 ex; UFRJ 8492, 4 ex, UFRJ 8495, 1 ex, UFRJ 8496, 1 ex, UFRJ 8920, 22 ex, Rio Boa Esperança basin, Nova Iguaçu, RJ, 22°36'58" S 43°25'52" W; UFRJ 700, 3 ex, UFRJ 1102, 1 ex (C&S), UFRJ 7371, 2 ex, UFRJ 8497, 4 ex, UFRJ 8501, 4 ex, UFRJ 8502, 5 ex, UFRJ 10648, 2 ex (C&S), UFRJ 12458, 1 ex, Rio Macacu basin, Cachoeiras de Macacu, RJ, 22°27' S 42°39' W; UFRJ 5722, 3 ex, UFRJ 5723, 19 exs, UFRJ 7736, 3 ex, UFRJ 7737, 7 ex, UFRJ 8473, 3 ex, UFRJ 8474, 6 ex, Rio Macacu basin, Cachoeiras de Macacu, RJ, 22°26'24" S 42°45'43" W; UFRJ 7370, 5 ex, Rio Macacu basin, Cachoeiras de Macacu, RJ, 22°24'57" S 42°36'29" W; UFRJ 5643, 24 ex, UFRJ 5664, 1 ex, UFRJ 5563, 1 ex (C&S), UFRJ 5417, 1 ex (C&S), UFRJ 5419, 2 ex (C&S), UFRJ 8469, 7 ex, UFRJ 7640, 3 ex, UFRJ 10646, 2 ex, Rio Macacu basin, Guapimirim, RJ, 22°29' S 43°00' W; UFRJ 8622, 1 ex, Rio Guapimirim basin, Guapimirim, RJ, 22°31'16" S 42°58'46" W; UFRJ 1643, 2 ex, UFRJ 5662, 1 ex, UFRJ 5703, 2 ex, UFRJ 5704, 1 ex (C&S), Baía da Ilha grande basin, Paraty, RJ, 23°13'10" S 44°43'0" W; UFRJ 5661, 4 ex, Rio Perequê-Açú, Parati basin, Paraty, RJ, 23°13'10" S 44°43'0" W; UFRJ 8206, 12 ex, Rio Grande basin, Rio de Janeiro, RJ 22°56'01" S 43°26'35" W; UFRJ 5321, 8, Rio Ribeira do Iguape basin, Iporanga, SP, 24°35'18" S 48°35'38" W; UFRJ 4549, 5 (C&S), Rio Ribeira do Iguape basin, Iguape, SP, 24°41'47" S 47°33'52" W; UFRJ 7626, 20, Rio Ribeira do Iguape basin, Miracatu, SP, 24°14'43" S 47°27'20" W; UFRJ 7627, 22, Rio Ubatumirim basin, 23°23'01" S 45°07'18" W; UFRJ 7628, 20, Rio Boiaçu basin, São Sebastião, SP, 23°45'43" S 45°36'25" W; UFRJ 12186, 10, UFRJ 12550, 7, Rio Ribeira do Iguape basin, Sete Barras, SP, 24°11'35" S 47°53'25" W; UFRJ 12757 19, Rio Ribeira do Iguape basin, Cajati, SP, 24°48'08" S 48°13'47" W UFRJ 5702, 3 (C&S), Rio da Guarda basin, Angra dos Reis, RJ, 23°00' S 44°19' W; UFRJ 5707, 3. *Trichomycterus aff. jacupiranga*: 5708, 2 (C&S), UFRJ 5717, 2, UFRJ 7638, 1, Rio Macabu basin, Conceição de Macabú, RJ, 22°04'36" S 41°57'48" W; UFRJ 5724, 3, UFRJ 5725, 12, UFRJ 3331, 5, UFRJ 5719, 2 (C&S), UFRJ 4485, 1, Rio São João basin, Silva Jardim, RJ, 22°39' S 42°23' W; UFRJ 5467, 1, UFRJ 5726, 1 (C&S), UFRJ 12710, 2, Rio Macaé basin, Macaé, RJ, 22°19' S 42°11' W; UFRJ 4119, 4, UFRJ 7620, 1 ex, Rio Macaé basin, Casimiro de Abreu, RJ, 22°28' S 42°12' W. *Trichomycterus jequitinhonhae Triques & Vono, 2004*: UFRJ 8229, 6; UFRJ 13138, 1 (C&S); Rio Jequitinhonha basin, Itaobim, MG, 16°31'19" S 41°30'05" W. *Trichomycterus largoperculatus Costa & Katz, 2022*: UFRJ 6987, P, UFRJ 6988, 7 P, UFRJ 6989, 3 P (C&S), CICC AA 02695, 2 P, Rio Paraíba do Sul, Além Paraíba, RJ, 21°50'36" S, 42°34'46" W. *Trichomycterus longibarbatatus Costa, 1992*: MZUSP 43339, H, UFRJ 629, 1 P; UFRJ 3368, 8 ex, UFRJ 5674, 3 ex (C&S), UFRJ 7236, 6 ex, UFRJ 9578, 2 ex, Rio Doce basin, Santa Teresa, ES, 19°55' S 40°35' W; UFRJ 13228, 3; UFRJ 13223, 1; Rio Doce basin, Santa Teresa, ES, 19°56' S 40°36' W. *Trichomycterus macrophthalmus*

**Barbosa & Costa, 2012:** UFRJ 6003, P, UFRJ 5683, 6 P, UFRJ 5675, 3 P (C&S), Rio Paraíba do Sul basin, Rio Claro, RJ, 22°40' S 44°02' W; UFRJ 12101, 1, Rio Pirai drainage, Rio Claro, RJ, 22°49' S 44°11' W UFRJ 12104, 1, Rio Pirai drainage, Rio Claro, RJ, 22°50' S 44°11' W. **Trichomycterus melanopygius Reis, Santos, Britto, Volpi & Pinna, 2020:** UFRJ 13130, 1, UFRJ 13136, 8, Rio Doce basin, Conceição do Mato Dentro, MG, 19°01' S 43°35' W; UFRJ 13242, 8, UFRJ 13226, 1 (C&S), Rio Doce basin, Rio Doce, MG, 20°11'44" S 42°51'56" W; UFRJ 13221, 1; Rio Doce basin, Iuna, ES, 20°20'34" S 41°32'41" W. **Trichomycterus mimosensis Barbosa, 2013:** UFRJ 8156, H, UFRJ 7545, 11, UFRJ 7792, 5 (C&S), Rio Itabapoana basin, Mimoso do Sul, ES, 21°03' S 41°18' W. **Trichomycterus pantherinus Alencar & Costa, 2004:** UFRJ 6001, P, UFRJ 5659, 22 P, UFRJ 5660, 6 P (C&S), Rio Santa Maria da Vitória basin, Município de Santa Leopoldina, 20°03'16" S 40°32'21" W; UFRJ 13243, 16; Rio Reis Magos basin, Santa Teresa, ES, 19°55'09" S 40°27'50" W. **Trichomycterus pradensis Sarmento-Soares, Martins-Pinheiro, Aranda & Chamon, 2005:** UFRJ 9743, 17, Rio dos Frades basin, Trancoso, BA, 16°38'03" S 39°08'09" W; UFRJ 9745, 6, UFRJ 10920, 1 (C&S), Rio Jucuruçu basin, Itamaraju, BA, 17°02'57" S 39°32'05" W; UFRJ 10411, 41, Rio Buranhém basin, BA, 16°34'45" S 40°06'15" W. **Trichomycterus puriventris** Barbosa & Costa, 2021: UFRJ 6005, H, UFRJ 5644, 1 P, UFRJ 5677, 1 P (C&S), Rio Paraíba do Sul basin, Santa Maria Madalena, RJ, 21°56'49" S 41°58'04" W; UFRJ 5397, 23 P, UFRJ 5398, 28 P, UFRJ 5405, 6 P, UFRJ 5624, 3 P, UFRJ 8432, 5 P (C&S), UFRJ 5687, 10 P, Rio Paraíba do Sul basin, Santa Maria Madalena, RJ, 21°54'14" S 41°57'25" W. **Trichomycterus tete** Barbosa & Costa, 2011: UFRJ 8062, H, UFRJ 7775, 9 P, UFRJ 7774, 3 P, UFRJ 7776, 8, Rio de Contas basin, Rio de Contas, BA, 13°29'45" S 41°53'05" W. **Trichomycterus travassosi (Miranda Ribeiro, 1949):** MNRJ 5424, H, UFRJ 596, 8, UFRJ 4554, 3 (C&S), UFRJ 4563, 1 (C&S), UFRJ 5140, ex, UFRJ 5354, 4 (C&S), UFRJ 5671, 8, UFRJ 12603, 2, Rio Paraíba do Sul basin, Resende, RJ, 22°26' S 44°30' W; UFRJ 5670, 3, Rio Paraíba do Sul basin, Itatiaia, RJ, 22°28'25" S 44°34'49" W. UFRJ 5246, 13, Rio Paraíba do Sul basin, São José do Barreiro, SP, 22°40' S 44°34' W. **Trichomycterus vinnulus Reis & de Pinna, 2022:** UFRJ 12790, 19; UFRJ 13240, 11; UFRJ 13241, 9; UFRJ 12998, 3 (C&S); Rio Doce basin, Rio Doce, MG, 20°11'44" S 42°51'56" W.

## Appendix B

**Table A1.** Terminal taxa for molecular phylogeny and respective GenBank accession numbers.

	COX1	CYTb	MYH6	RAG2
<i>Nematogenys inermis</i>	KY857952	-	KY858107	KY858182
<i>Copionodon pecten</i>	KY857929	-	KY858084	KY858169
<i>Trichogenes longipinnis</i>	MK123682	MK123704	MF431104	MF431117
<i>Microcambeva ribeirae</i>	MN385807	OK334290	MN385819	MN385832
<i>Listrura tetraradiata</i>	MN385804	JQ231088	MN385814.1	MN385826.1
<i>Eremophilus mutisii</i>	KY857931	-	KY858086	KY858171
<i>Ituglanis boitata</i>	MK123684	MK123706	MF431105	MK123758
<i>Bullockia maldonadoi</i>	KY857926	FJ772237	KY858081	KY858166
<i>Scleronema minutum</i>	MK123685	MK123707	MK123735.1	MK123759.1
<i>Cambeva barbosae</i>	MK123689	MK123713	MK123740.1	MN385820
<i>Trichomycterus itaiayae</i>	MW671552	MW679291	KY858128	KY858198
<i>Trichomycterus reinhardti</i>	MK123698	MK123727	MF431106	MF431119

**Table A1.** Cont.

	COX1	CYTB	MYH6	RAG2
<i>Trichomycterus giganteus</i>	MK123693	MK123720	MK123746	MT446426
<i>Trichomycterus nigricans</i>	MN813005	MK123723	MK123750	MK123765
<i>Trichomycterus nigroauratus</i>	MK123696	MK123724	MK123751	MK123766
<i>Trichomycterus albinotatus</i>	MN813007	MK123716	MK123743	MN812990
<i>Trichomycterus brasiliensis</i>	MK123691	MK123717	MK123744	MK123763
<i>Trichomycterus mimonha</i>	MW196749	MW196758	MW196770	MW196783
<i>Trichomycterus mirissumba</i>	MW196752	MW196761	MW196773	MW196786
<i>Trichomycterus caudofasciatus</i>	MN812995	MK123719	MK123719	MK123764
<i>Trichomycterus jacupiranga</i>	MK123702	MK123731.1	MK123757	OP688469
<i>Trichomycterus pantherinus</i>	MK123697	MK123725	MK123752	MN812989
<i>Trichomycterus pradensis</i>	MN813003	MK123726	MK123753	MN812988
<i>Trichomycterus goeldii</i>	MT435136	MT436453	MT436451	MT446427
<i>Trichomycterus alternatus</i>	MK123690	MK123715	MK123742	MN812991.1
<i>Trichomycterus melanopygius</i>	KY857976	KY858045	KY858127	KY858197
<i>Trichomycterus astromycterus</i>	ON036881	OK652453	OK652451.1	OK652448.1
<i>Trichomycterus saquarema</i>	OP698258	OP688464	-	OP688470
<i>Trichomycterus macrophthalmus</i>	OL741727	OL752426	-	OL752421
<i>Trichomycterus travassosi</i>	MK123701	MK123730	MK123757	OL752425
<i>Trichomycterus auroguttatus</i>	MT435135	MT436452	MT436450	OP699434
<i>Trichomycterus puriventris</i>	OP698259	OP688465	OP688467	OP688471
<i>Trichomycterus vinnulus</i>	-	OK652452	OK652450	OK652449
<i>Trichomycterus altipombensis</i>	OP698260	OP688466	OP688468	OP688472

## Appendix C

**Table A2.** Best-fitting partition schemes and evolutive models.

Partition	Base pairs	Evolutive Model
COX1 1st	174	TIM + I + G
COX1 2nd	174	HKY + I
COX1 3rd	174	TRN + G
CYTB 1st	363	K80 + I + G
CYTB 2nd	363	TIM + I
CYTB 3rd	362	GTR + I + G
MYH6 1st	181	TRN + I + G
MYH6 2nd	181	TRN + I + G
MYH6 3rd	181	K80 + G
RAG2 1st	274	K81 + I + G
RAG2 2nd	274	TVM + G
RAG2 3rd	273	K80 + G

Appendix D

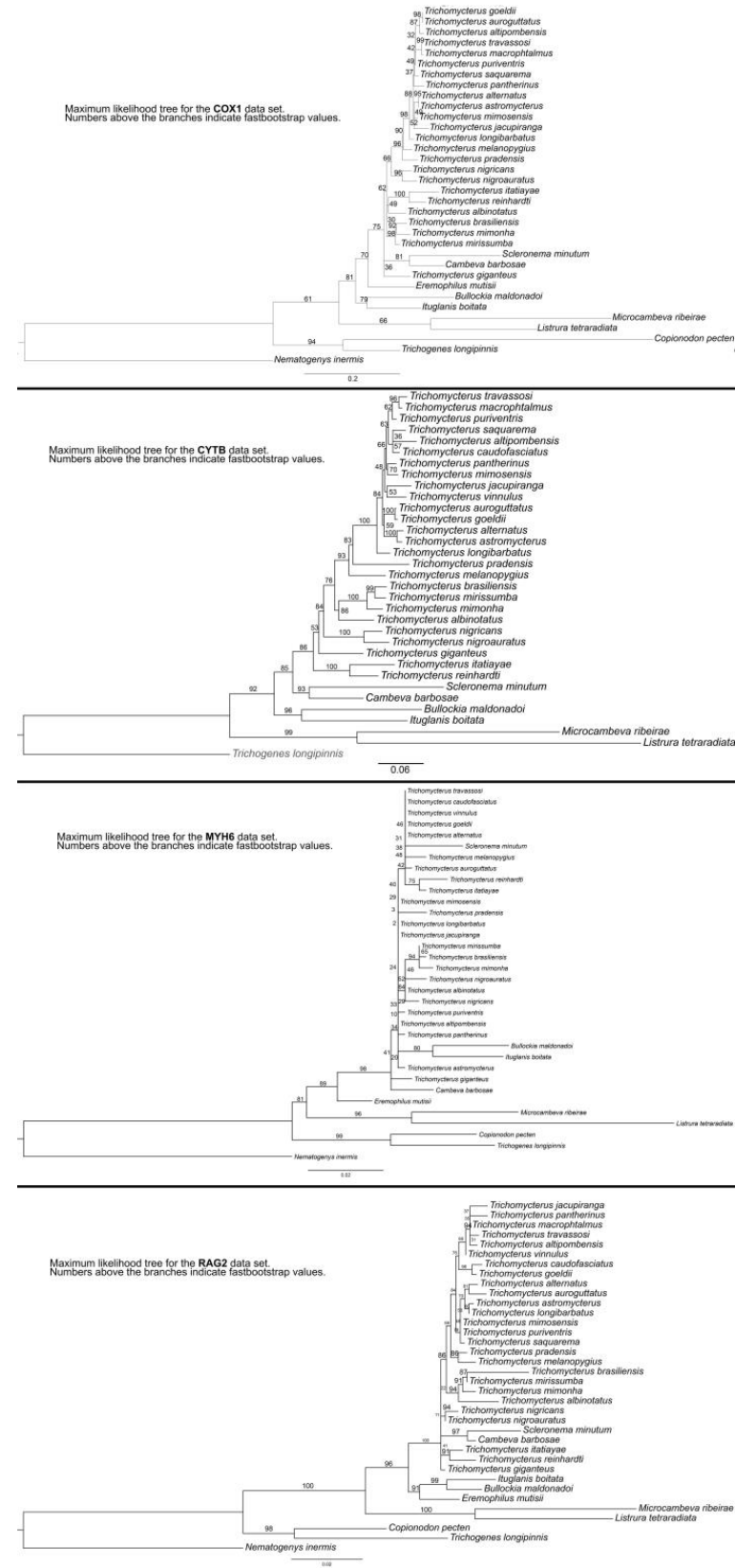


Figure A1. Genes trees generated by IQTree.

## References

1. Katz, A.M.; Barbosa, M.A.; Mattos, J.L.O.; Costa, W.J.E.M. Multigene analysis of the catfish genus *Trichomycterus* and description of a new South American trichomycterine genus (Siluriformes, Trichomycteridae). *Zoosystematics Evol.* **2018**, *94*, 557–566. [CrossRef]
2. Ochoa, L.E.; Datovo, A.; DoNascimento, C.; Roxo, F.F.; Sabaj, M.H.; Chang, J.; Melo, B.F.; Silva Gabriel, S.C.; Foresti, F.; Alfaro, M.; et al. Phylogenomic analysis of trichomycterid catfishes (Teleostei: Siluriformes) inferred from ultraconserved elements. *Sci. Rep.* **2020**, *10*, 2697. [CrossRef] [PubMed]
3. Fricke, R.; Eschmeyer, W.N.; Van der Laan, R. Eschmeyer's Catalog of Fishes: Genera, Species, References. 2022. Available online: <http://researcharchive.calacademy.org/research/ichthyology/catalog/fishcatmain.asp> (accessed on 3 December 2022).
4. Eigenmann, C.H. The Pygidiidae, a subfamily of South American catfishes. *Mem. Carnegie Mus.* **1918**, *7*, 259–398. [CrossRef]
5. Hayes, M.M.; Paz, H.J.; Stout, C.C.; Werneke, D.C.; Armbruster, J.W. A hotspot atop: Rivers of the Guyana Highlands hold high diversity of endemic pencil catfish (Teleostei: Ostariophysi: Siluriformes). *Biol. J. Linn. Soc.* **2020**, *129*, 862–874. [CrossRef]
6. Costa, W.J.E.M.; Mattos, J.L.O.; Katz, A.M. Two new catfish species from central Brazil comprising a new clade supported by molecular phylogeny and comparative osteology (Siluriformes: Trichomycteridae). *Zool. Anz.* **2021**, *293*, 124–137. [CrossRef]
7. Costa, W.J.E.M. Comparative osteology, phylogeny and classification of the eastern South American catfish genus *Trichomycterus* (Siluriformes: Trichomycteridae). *Taxonomy* **2021**, *1*, 160–191. [CrossRef]
8. Costa, W.J.E.M.; Mattos, J.L.O.; Katz, A.M. Phylogenetic position of *Trichomycterus payaya* and examination of osteological characters diagnosing the Neotropical catfish genus *Ituglanis* (Siluriformes: Trichomycteridae). *Zool. Stud.* **2021**, *60*, 43. [CrossRef]
9. Costa, W.J.E.M.; Sampaio, W.M.S.; Giongo, P.; de Almeida, F.B.; Azevedo-Santos, V.M.; Katz, A.M. An enigmatic interstitial trichomycterine catfish from south-eastern Brazil found at about 1000 km away from its sister group (Siluriformes: Trichomycteridae). *Zool. Anz.* **2022**, *297*, 85–96. [CrossRef]
10. Vilardo, P.J.; Katz, A.M.; Costa, W.J.E.M. Phylogenetic position of *Trichomycterus astromycterus* (Siluriformes: Trichomycteridae), an enigmatic trichomycterid from eastern Brazil, inferred from molecular data. *J. Fish Biol.* **2022**, *100*, 1093–1096. [CrossRef]
11. Costa, W.J.E.M.; Mattos, J.L.O.; Amorim, P.F.; Vilardo, P.J.; Katz, A.M. Relationships of a new species support multiple origin of melanism in *Trichomycterus* from the Atlantic Forest of south-eastern Brazil (Siluriformes: Trichomycteridae). *Zool. Anz.* **2020**, *288*, 74–83. [CrossRef]
12. Myers, N.; Mittermeir, R.A.; Mittermeir, C.G.; da Fonseca, G.A.B.; Kent, J. Biodiversity hotspots for conservation priorities. *Nature* **2000**, *403*, 853–858. [CrossRef] [PubMed]
13. Costa, W.J.E.M.; Katz, A.M. A new catfish of the genus *Trichomycterus* from the Rio Paraíba do Sul Basin, south-eastern Brazil, a supposedly migrating species (Siluriformes, Trichomycteridae). *Zoosystematics Evol.* **2022**, *98*, 13–21. [CrossRef]
14. Sanjad, N. *Emílio Goeldi (1859–1917): A ventura de um naturalista entre a Europa e o Brasil*; EMC Edições: Rio de Janeiro, Brazil, 2009; 232p.
15. Boulenger, G.A. Description of a new siluroid fish from the Organ Mountains, Brazil. *Ann. Mag. Nat. Hist.* **1896**, *18*, 154. [CrossRef]
16. Miranda Ribeiro, P. Duas novas espécies de peixes na coleção ictiológica do Museu Nacional (Pisces, Callichthyidae et Pygidiidae). *Rev. Bras. De Biol.* **1949**, *9*, 143–145.
17. Costa, W.J.E.M. Description de huit nouvelles espèces du genre *Trichomycterus* (Siluriformes: Trichomycteridae), du Brésil oriental. *Rev. Française D'aquariologie Et Herpetol.* **1992**, *18*, 101–110.
18. Barbosa, M.A.; Costa, W.J.E.M. *Trichomycterus macrophthalmus* (Teleostei: Siluriformes: Trichomycteridae), a new species of catfish from the rio Paraíba do Sul basin, southeastern Brazil. *Vertebr. Zool.* **2012**, *62*, 79–82.
19. Barbosa, M.A.; Costa, W.J.E.M. *Trichomycterus puriventris* (Teleostei: Siluriformes: Trichomycteridae), a new species of catfish from the rio Paraíba do Sul basin, southeastern Brazil. *Vertebr. Zool.* **2012**, *62*, 155–160.
20. Reis, V.J.C.; de Pinna, M.C.C. The type specimens of *Trichomycterus alternatus* (Eigenmann, 1917) and *Trichomycterus zonatus* (Eigenmann, 1918), with elements for future revisionary work (Teleostei: Siluriformes: Trichomycteridae). *Zootaxa* **2019**, *4585*, 100–120. [CrossRef]
21. Reis, V.J.C.; de Pinna, M.C.C. Diversity and systematics of *Trichomycterus Valenciennes 1832* (Siluriformes: Trichomycteridae) in the Rio Doce Basin: Iterating DNA, phylogeny and classical taxonomy. *Zool. J. Linn. Soc.* **2022**. [CrossRef]
22. Vilardo, P.J.; Katz, A.M.; Costa, W.J.E.M. Relationships and description of a new species of *Trichomycterus* (Siluriformes: Trichomycteridae) from the Rio Paraíba do Sul basin, south-eastern Brazil. *Zool. Stud.* **2020**, *59*, 53. [CrossRef]
23. Leary, S.; Underwood, W.; Anthony, R.; Cartner, S.; Corey, D.; Grandin, T.; Greenacre, C.; Gwaltney-Brant, S.; McCrackin, M.; Meyer, R.; et al. AVMA Guidelines for the Euthanasia of Animals: 2020 Edition. 2020. Available online: <http://www.avma.org/sites/default/files/2020-02/Guidelines-on-Euthanasia-2020.pdf> (accessed on 3 December 2022).
24. Close, B.; Banister, K.; Baumans, V.; Bernoth, E.M.; Bromage, N.; Bunyan, J.; Erhardt, W.; Flecknell, P.; Gregory, N.; Hackbarth, H.; et al. Recommendations for euthanasia of experimental animals: Part 1. *Lab. Anim.* **1996**, *30*, 293–316. [CrossRef] [PubMed]
25. Close, B.; Banister, K.; Baumans, V.; Bernoth, E.M.; Bromage, N.; Bunyan, J.; Erhardt, W.; Flecknell, P.; Gregory, N.; Hackbarth, H.; et al. Recommendations for euthanasia of experimental animals: Part 2. *Lab. Anim.* **1997**, *31*, 1–32. [CrossRef] [PubMed]
26. Costa, W.J.E.M.; Katz, A.M.; Mattos, J.L.O.; Amorim, P.F.; Mesquita, B.O.; Vilardo, P.J.; Barbosa, M.A. Historical review and redescription of three poorly known species of the catfish genus *Trichomycterus* from south-eastern Brazil (Siluriformes: Trichomycteridae). *J. Nat. Hist.* **2020**, *53*, 2905–2928. [CrossRef]



27. Bockmann, F.A.; Sazima, I. *Trichomycterus maracaya*, a new catfish from the upper rio Paraná, southeastern Brazil (Siluriformes: Trichomycteridae), with notes on the *T. brasiliensis* species-complex. *Neotrop. Ichthyol.* **2004**, *2*, 61–74. [[CrossRef](#)]
28. Taylor, W.R.; Van Dyke, G.C. Revised procedures for staining and clearing small fishes and other vertebrates for bone and cartilage study. *Cybium* **1985**, *9*, 107–119.
29. Arratia, G.; Huaquin, L. Morphology of the lateral line system and of the skin of diplomystic and certain primitive loricarioid catfishes and systematic and ecological considerations. *Bonn Zool. Monogr.* **1995**, *36*, 1–110.
30. Villa-Verde, L.; Lazzarotto, H.; Lima, S.Q.M. A new glanapterygine catfish of the genus *Listrura* (Siluriformes: Trichomycteridae) from southeastern Brazil, corroborated by morphological and molecular data. *Neotrop. Ichthyol.* **2012**, *10*, 527–538. [[CrossRef](#)]
31. Unmack, P.J.; Bennin, A.P.; Habi, E.M.; Victoriano, P.F.; Johnson, J.B. Impact of ocean barriers, topography, and glaciation on the phylogeography of the catfish *Trichomycterus areolatus* (Teleostei: Trichomycteridae) in Chile. *Biol. J. Linn. Soc.* **2009**, *97*, 876–892. [[CrossRef](#)]
32. Barros, L.C.; Santos, U.; Cioffi, M.D.B.; Dergam, J.A. Evolutionary divergence among *Oligosarcus* spp. Ostariophysi, Characidae from the São Francisco and Doce River Basins: *Oligosarcus solitarius* Menezes, 1987 shows the highest rates of chromosomal evolution in the Neotropical region. *Zebrafish* **2015**, *12*, 102–110. [[CrossRef](#)]
33. Ward, R.D.; Zemlak, T.S.; Innes, B.H.; Last, P.R.; Hebert, P.D. DNA barcoding Australia’s fish species. *Philos. Trans. R. Soc. Lond. B Biol. Sci.* **2005**, *360*, 1847–1857. [[CrossRef](#)]
34. Hardman, M.; Page, L.M. Phylogenetic relationships among bullhead catfishes of the genus *Ameiurus* (Siluriformes: Ictaluridae). *Copeia* **2003**, *2003*, 20–33. [[CrossRef](#)]
35. Costa, W.J.E.M.; Henschel, E.; Katz, A.M. Multigene phylogeny reveals convergent evolution in small interstitial catfishes from the Amazon and Atlantic forests (Siluriformes: Trichomycteridae). *Zool. Scr.* **2020**, *49*, 159–173. [[CrossRef](#)]
36. Cramer, C.A.; Bonatto, S.L.; Reis, R.E. Molecular phylogeny of the Neoplecostominae and Hypoptopomatinae (Siluriformes: Loricariidae) using multiple genes. *Mol. Phylogenetics Evol.* **2011**, *59*, 43–52. [[CrossRef](#)] [[PubMed](#)]
37. Li, C.; Ortí, G.; Zhang, G.; Lu, G. A practical approach to phylogenomics: The phylogeny of ray-finned fish (Actinopterygii) as a case study. *BMC Evol. Biol.* **2007**, *7*, 44. [[CrossRef](#)]
38. Tamura, K.; Stecher, G.; Kumar, S. MEGA11: Molecular Evolutionary Genetics Analysis Version 11. *Mol. Biol. Evol.* **2021**, *38*, 3022–3027. [[CrossRef](#)] [[PubMed](#)]
39. Chenna, R.; Sugawara, H.; Koike, T.; Lopez, R.; Gibson, T.J.; Higgins, D.G.; Thompson, J.D. Multiple sequence alignment with the Clustal series of programs. *Nucleic Acids Res.* **2003**, *31*, 3497–3500. [[CrossRef](#)]
40. Lanfear, R.; Frandsen, P.B.; Wright, A.M.; Senfeld, T.; Calcott, B. PartitionFinder 2: New methods for selecting partitioned models of evolution for molecular and morphological phylogenetic analyses. *Mol. Biol. Evol.* **2017**, *34*, 772–773. [[CrossRef](#)]
41. Ronquist, F.; Teslenko, M.; van der Mark, P.; Ayres, D.L.; Darling, A.; Höhna, S.; Larget, B.; Liu, L.; Suchard, M.A.; Huelsenbeck, J.P. MrBayes 3.2: Efficient Bayesian phylogenetic inference and model choice across a large model space. *Syst. Biol.* **2012**, *61*, 539–542. [[CrossRef](#)]
42. Rambaut, A.; Drummond, A.J.; Xie, D.; Baele, G.; Suchard, M.A. Posterior summarisation in Bayesian phylogenetics using Tracer 1.7. *Syst. Biol.* **2018**, *67*, 901–904. [[CrossRef](#)]
43. Nguyen, L.T.; Schmidt, H.A.; von Haeseler, A.; Minh, B.Q. IQ-TREE: A fast and effective stochastic algorithm for estimating maximum likelihood phylogenies. *Mol. Biol. Evol.* **2015**, *32*, 268–274. [[CrossRef](#)]
44. Minh, B.Q.; Nguyen, M.A.T.; von Haeseler, A. Ultrafast approximation for phylogenetic bootstrap. *Mol. Biol. Evol.* **2013**, *30*, 1188–1195. [[CrossRef](#)] [[PubMed](#)]
45. Felsenstein, J. Confidence limits on phylogenies: An approach using the bootstrap. *Evolution* **1985**, *39*, 783–791. [[CrossRef](#)] [[PubMed](#)]
46. Costa, W.J.E.M. Feeding habits of a fish community in a tropical coastal stream, Rio Mato Grosso, Brazil. *Stud. Neotrop. Fauna Environ.* **1987**, *22*, 145–153. [[CrossRef](#)]
47. Donin, L.M.; Ferrer, J.; Carvalho, T.P. Taxonomical study of *Trichomycterus* (Siluriformes: Trichomycteridae) from the Ribeira de Iguape River basin reveals a new species recorded in the early 20th century. *J. Fish Biol.* **2020**, *96*, 886–904. [[CrossRef](#)] [[PubMed](#)]
48. Lima, S.M.Q.; Berbel-Filho, W.M.; Vilasboa, A.; Lazoski, C.; Volpi, T.A.; Lazzarotto, H.; Russo, C.A.M.; Tatarenkov, A.; Avise, J.C.; Solé-Cava, A.M. Rio de Janeiro and other palaeodrainages evidenced by the genetic structure of an Atlantic Forest catfish. *J. Biogeogr.* **2021**, *48*, 1475–1488. [[CrossRef](#)]
49. Wosiacki, W.B.; Oyakawa, O.T. Two new species of the catfish genus *Trichomycterus* (Siluriformes: Trichomycteridae) from the rio Ribeira de Iguape Basin, Southeastern Brazil. *Neotrop. Ichthyol.* **2005**, *3*, 465–472. [[CrossRef](#)]
50. Bizerril, C.R.S.F.; Primo, P.B.S. *Peixes de águas interiores do estado do Rio de Janeiro*; Secretaria de Estado de Meio Ambiente e Desenvolvimento Sustentável; Fundação de Estudos do Mar: Rio de Janeiro, Brazil, 2001; 417p.
51. Bizerril, C.R.S.F.; Araujo, L.M.N.; Tosin, P.C. (Eds.) *Contribuição ao conhecimento da bacia do Rio Paraíba do Sul: Coletânea de estudos*; Agência Nacional de Energia Elétrica: Brasília, Brazil, 1998; 113p.
52. Polaz, C.N.M.; Bataus, Y.S.L.; Desbiez, A.; Reis, M.L. *Plano de ação nacional para a conservação das espécies aquáticas ameaçadas de extinção da bacia do Rio Paraíba do Sul. Série Espécies Ameaçadas 16*; Instituto Chico Mendes de Conservação da Biodiversidade: Brasília, Brazil, 2011; 140p.
53. Costa, W.J.E.M.; Katz, A.M. Integrative taxonomy supports high species diversity of south-eastern Brazilian mountain catfishes of the *T. reinhardti* group (Siluriformes: Trichomycteridae). *Syst. Biodivers.* **2021**, *19*, 601–621. [[CrossRef](#)]